Atmospheric Research 127 (2013) 154–177

Contents lists available at SciVerse ScienceDirect

Atmospheric Research

journal homepage: www.elsevier.com/locate/atmos

Spring and summer extreme temperatures in Iberia during last century in relation to circulation types

Sonia Fernández-Montes [a,*], Fernando S. Rodrigo [a], Stefanie Seubert [b], Pedro M. Sousa [c]

[a] *University of Almeria, Applied Physics, Almería, Spain*
[b] *University of Augsburg, Institute of Geography, Augsburg, Germany*
[c] *University of Lisbon, CGUL, IDL, Lisbon, Portugal*

ARTICLE INFO

Article history:
Received 16 December 2011
Received in revised form 13 June 2012
Accepted 14 July 2012

Keywords:
Iberian extreme temperatures
Circulation types
Sea level pressure
Spring and summer warming
Within-type changes

ABSTRACT

In the Iberian Peninsula the raise of temperatures has been notable from mid-1970s to mid-2000s, especially in spring and summer. This study analyses spatial and temporal relationships between extreme temperatures and atmospheric circulation types (CTs) defined over the Iberian Peninsula (IP) in these seasons. Station series (29) of maximum and minimum temperature are considered, starting from 1905 until 2006. The CTs (9 for spring and 8 for summer) are derived by a cluster method applied to daily mean SLP grids covering the period 1850–2003. Changes in the seasonal frequency of extreme temperatures and of CTs are analysed. Subsequently, the CTs are examined for their effectiveness in leading to moderately extreme temperatures (at each location) using an index that measures the contribution to extreme days with respect to the contribution to non-extreme days. Correlation between regional extreme series and CTs frequency is also tested.

In spring, the decrease in cold nights, which is notable in the 1970s onwards, can be partially attributable to a downtrend in the frequency of Northerly flow. High frequency of Anticyclone in North Iberia in the 1980s and 1990s has contributed to an increase in warm days in West and North stations. To the SE quadrant of the IP, a great part of warm days is related to south-westerly flow, (both) presenting a higher frequency in the 1950s and the 1960s.

In summer warm nights increased remarkably to the SE and SW, and may be in part related to uptrends in Iberian thermal low pattern (1950–2003) and North Atlantic Anticyclone (1850–2003) respectively. Warm days have increased remarkably to the NE especially in the 1990s and 2000s, but this is not found to be related to changes in CTs' frequency.

Furthermore, the existence of within type changes (variations in Tmax, Tmin and extreme indices within the CTs) points to the identification of other physical factors operating on inter-annual to multidecadal time scales. Thus, the consideration of Sea Surface Temperature (SST) of the East Atlantic Ocean and Iberian soil moisture conditions (by means of a drought index) helps to explain the evolution of extreme temperatures.

1. Introduction

The summer heatwaves of 2003 and 2010 broke records for intensity, duration and extension of high temperatures respectively in West (Schar et al., 2004) and East Europe (Barriopedro et al., 2011). From a long-term perspective, greenhouse warming has very likely influenced temperatures and increased temperature variability in Europe (ibid.), leading in general to more frequent and hitter warm extremes and to an attenuation of cold events (e.g., Moberg et al., 2006). Given that atmospheric dynamics is the main driver of regional climate changes at mid-latitudes (e.g., Jacobeit et al., 2003; Xoplaki et al., 2003), it is essential to analyse whether circulation patterns have also changed in frequency favouring a shift towards warmer conditions. Thus, it is necessary to discover to what

* Corresponding author. Tel.: +34 950214158; fax: +34 950015477.
E-mail address: soniafm@ual.es (S. Fernández-Montes).

0169-8095/$ – see front matter
doi:10.1016/j.atmosres.2012.07.013

extent fluctuations in extreme temperatures can be explained by circulation variability, e.g., in terms of circulation indices (Slonosky et al., 2001; Cattiaux et al., 2010), or circulation types (Domonkos et al., 2003; Maheras et al., 2006 for Eastern Mediterranean). And at the same time, it is crucial to find out whether the link between surface circulation and climate is affected by other factors (shown for Europe by Küttel et al., 2010; Jones and Lister, 2009), e.g., by anthropogenic global warming. Hence, even if dynamic conditions leading to extreme temperatures probably remain the same, they fail to capture the amplitude of recent European anomalous seasons (Cattiaux et al., 2010, 2011).

Understanding the mechanisms influencing extreme temperatures in the long-term is essential for Mediterranean regions, characterized by a large natural variability and vulnerability to extreme conditions. The Iberian Peninsula (IP) is highly affected by the general circulation of the atmosphere. It is situated in the mid-latitude belt with a predominance of westerly circulation which brings both subtropical and polar (both maritime and continental) air masses, and it stands as a transitional zone between wet and dry climates (northwest to southeast gradient). Iberian climate is also under the influence of the Atlantic Ocean and the Mediterranean Sea as sources of water and heat exchange, and important land-atmosphere processes at the regional scale (e.g., Jerez et al., 2010, 2012). Therefore, temperatures in the IP present a great spatial variability, and geographical (regional and/or local) factors play an important role in conjunction with the direction, intensity, temperature and moisture of the atmospheric flow (e.g., Rasilla, 2003; Rasilla et al., 2010).

North-Atlantic atmospheric dynamics is a main factor controlling European land temperatures and cold and hot events (Cassou et al., 2005). A comprehensive work by Della-Marta et al. (2007) found that large-scale circulation forcing can account up to a 35% of Western Europe summer heat-waves variability from 1880 to 2003. They found that the statistical skill substantially improved by considering Sea Surface Temperatures (hereafter SSTs) and soil moisture conditions (via precipitation). Thus, added to atmospheric dynamics, the influence of SSTs (Rodriguez-Puebla et al., 2010; Feudale and Shukla, 2010), soil moisture anomalies and other radiative effects (aerosols, clouds, GHG) are usually necessary to fully explain extremely anomalous temperatures (Ferranti and Viterbo, 2005; Barriopedro et al., 2011; Cattiaux et al., 2010). A soil moisture deficit limits evaporation and increases sensible heat flux, raising air temperatures, this coupling being important in transitional areas between wet and dry climates (Seneviratne et al., 2010; El Kenawy et al., 2011a; Jerez et al., 2010, 2012). Also drought conditions in the Mediterranean area may propagate and favour hot events further north (e.g., Zampieri et al., 2009). Additionally, land temperatures as well as SST anomalies influence atmospheric pressure conditions. For example, warm land conditions in summer over Iberia favour the generation of thermal lows.

Extreme temperatures in the IP have agricultural, environmental and human impacts and risks. Very low temperatures in spring have implications for energy consumption, ecosystems and agriculture (for example, frosts in spring damage to crops sprouts, such as grapes and olives). Extreme high temperature in early spring also damage crops and may result in enhanced sensitivity of plants to later cold spells (Domonkos et al. 2003). The impacts of high night-time temperatures are greater in summer, e.g., may enhance human stress and mortality. In summer the occurrence of high daytime temperatures has the greatest impact both on environment (e.g, fire hazards, Trigo et al., 2006) and human health (García-Herrera et al., 2005).

Focusing on long-term temperature changes in Spain, Brunet et al. (2007) found increases in warm extremes and decreases in cold extremes during the last century; moreover, they found that, for the recent period 1973–2005, both maximum (Tmax) and minimum (Tmin) temperatures have risen quickly and at similar rates (0.51 vs. 0.47 °C/decade), mainly due to spring and summer warming. For Portugal, the increase in extreme temperatures in 1976–2006 is also more remarkable in spring and summer (Ramos et al., 2011b). Using high spatial resolution for the NE Spanish quadrant (128 observatories) in 1960–2006, El Kenawy et al. (2011a) also found larger trends in spring and summer. El Kenawy et al. (2011b) reported more significant (annual) changes for warm than cold extremes, with the coastal areas along the Mediterranean Sea and the Cantabrian Sea (Biscay gulf) experiencing a stronger warming than inland areas. Also on an annual scale for 1950–2006, Rodriguez-Puebla et al. (2010) reported increasing trends in warm days, more pronounced to NE and SW of the IP, and a decrease in cold nights.

Iberian extreme temperatures have been related to northern hemisphere teleconnection patterns (Rodriguez-Puebla et al., 2010; Fernández-Montes and Rodrigo, 2011; El Kenawy et al., 2011a,b), such as the Scandinavian Pattern (Barnston and Livezey, 1987). However, in synoptic climatology a variety of classification methods (Huth et al., 2008) provide atmospheric circulation types (CTs) which can be analysed in their frequency and associated surface climate variables. CTs as averages of many individual daily pressure fields, besides offering a clear dynamical interpretation, usually represents well the surface meteorology, such as frontal temperature and precipitation changes (Philipp et al., 2007; Rasilla, 2003; Esteban et al., 2009). A number of studies have reported changes in CTs for the IP. For the period 1960–2001, Esteban et al. (2006) obtained significant trends in patterns of high frequency in summer and spring months, like a downtrend in patterns with northerly flow in Western Europe. For NW Iberia, Lorenzo et al. (2011) found uptrends in the frequency of cyclonic and south-westerly types in summer for the period 1948–2008, and uptrends (downtrends) in south-westerly (northerly) flow in spring over the period 1978–2008.

CTs usually provide a good characterization of precipitation in Iberia (among others, Goodess and Jones, 2002; Trigo and DaCamara, 2000; Lorenzo et al., 2008). Other meteorological applications comprise e.g., lightning activity (Ramos et al., 2011a) or fire hazards (Rasilla et al., 2010). A few studies have also analysed temperatures-CTs relationship for the IP. Thus, links between European CTs and stations mean temperature (Tmean) anomalies are partially described by Jones and Lister (2009), who compared three 30-year periods in 1911–2000 and found increases of Tmean in all seasons except autumn. Focussed on changes in 100 weather types for two sub-periods in the second half of 20th century, Bermejo and Ancell (2009) found increases of Tmax and Tmin in Spain within most types. However, the cited works did not analyse which synoptic circulations patterns are most conducive to temperature extremes.

Naturally, composites of atmospheric circulation fields from dates with extreme temperatures provide the best characterization of anomalous synoptic circulation, as did García-Herrera et al. (2005) for summer hot events at Lisbon and Madrid in 1958–1997. But then the analysis has to be focussed on one or few stations and temperature information of the remaining days and stations is missed.

The present study develops objective circulation classifications for the IP for spring and summer (all days) and applies them for first time in connection with Tmax and Tmin extreme indices for the whole IP (29 stations). The aim is to find out which changes in extreme temperatures are related to overall circulation changes. A motivation is that higher trends in extreme temperatures both in Portugal (Ramos et al., 2011b) and Spain (Brunet et al., 2007; El Kenawy et al., 2011a) have been detected within these seasons. A similar study was previously performed for winter (Fernández-Montes et al., 2012). The specific objectives are:

1) To study spatiotemporal variations in the occurrence of extreme temperatures that have a greater impact, i.e., warm days and cold nights in spring and warm days and nights in summer (for the shared period from 1947 to 2006).
2) To analyse long-term fluctuations (1850–2003) in characteristic atmospheric circulation types (CTs) in spring and summer over the Iberian Peninsula.
3) To identify the CTs most conducive to local extreme temperatures, and relate changes in extreme temperatures to changes in the frequency of those CTs.
4) To analyse within-type changes (Beck et al., 2007; Jacobeit et al., 2009) in mean temperatures and frequency of extremes. The presence of within-type signals could lead us to the identification of low-frequency physical mechanisms relevant for extreme temperatures, e.g., long-term memory factors such as SST or soil moisture anomalies (Seneviratne et al, 2010).

Section 2 describes the data, the methods for deriving the circulation types and for relating them to extreme temperatures. In Section 3 the results are presented. In Section 4 a discussion is presented and in Section 5 the most important conclusions from the work are highlighted.

2. Data and methods

2.1. Station temperature series and extreme indices

The database consists of long-term series of daily Tmin and Tmax for 29 stations across the Iberian Peninsula (see Table 1; Fig 1). This database presents a reasonably good spatial coverage. Table 1 shows the period of the series considered for the present work, with 23 stations covering the period 1905–2006. Most series come from the databases of Spanish Daily Adjusted Temperature series (SDATS), whose sources and homogeneity procedures are described by Brunet et al (2006, 2007). These data have undergone quality control (QC) and homogenization at the daily scale by following procedures similar to those described by the World Meteorological Organization/ World Climate Data Monitoring Programme Guidance on the development of daily adjusted temperature data sets (Brunet et al., 2008). Four series (PE, BR, L, and PO) from ECAD (Klein Tank et al., 2002; Klok and Klein Tank, 2009) have been added.

A simple additional QC was applied to the whole database by means of Rclimdex software ("http://cccma.seos.uvic.ca/ETCCDMI/RClimDex/rclimdex.r") to detect possible digitalizing or instrumental errors such as a) Daily Tmax below Tmin (no errors) and b) extreme values ("outliers") in Tmax and Tmin. The outliers are daily values that fall out of a region defined by the user, in our case, 4 times the Standard Deviation (STD) of the sample. In these cases we investigated (searching in newspapers, checking historical SLP maps) whether they likely refer to real registered extreme-values. Therefore we finally did not remove these potential outliers if we found corroborating documentary evidence.

The completeness was tested for all the series in a seasonal scale. The criterion applied by Moberg et al (2006) was taken:

- First each 3-month season (spring and summer for this work) is considered complete if there is no more than 3 missing days per season.
- Then each 20-year block from 1905 to 2006 was checked to have at least 10 complete years according to the rule above.

All stations are complete with more than 15 complete seasons per block. Considering overall missing data, the series with more missing values in spring (summer) are Albacete with around 9.2% (8.5%) of missing values in its whole period, Pamplona with 8.2% (9%), Huesca with 7.4% (6.4%), Valencia with 7% (6.3%) and Barcelona with 4.9 (5.4%). The rest of stations have less than 5% of missing days.

Daily extreme temperature indices are percentile-based, similar to indices defined by the Expert Team on Climate Change Detection, Monitoring and Indices (ETCCDMI, http://cccma.seos.uvic.ca/ETCCDMI/), which allow for comparison among different regions. We analyse the following indices:

- Cold nights (TN10p), as days on which Tmin falls below the station specific daily 10th percentile value of the reference period 1971–2000.
- Warm nights (TN90p), as days on which Tmin exceeds the station specific daily 90th percentile value of the reference period 1971–2000.
- Warm days (TX90p), as days on which Tmax exceeds the station specific daily 90th percentile value of the reference period 1971–2000.

Daily percentiles are defined by means of an 11-days window to account for the annual cycle of temperature. These defined indices are a compromise between Tmean 90th percentile –smoother than Tmax and Tmin 90th percentiles – and higher thresholds (e.g., 95th percentile) which could make the statistical method less robust since very few extremes could occur. The same indices have been used in several studies, e.g., in the Iberian Peninsula by Brunet et al. (2007), Rodriguez-Puebla et al. (2010), Ramos et al. (2011b), El Kenawy et al. (2011b).

2.2. Circulation data and classification method

We have used daily reconstructions of mean sea level pressure (SLP) from the Emulate project (European and North Atlantic daily to MULtidecadal climATE variability). The development and quality features of Emulate reconstructions are described in Ansel et al. (2006). They are built from a variety of

Table 1
Description of station series of daily maximum and minimum temperatures, latitude (LAT, in decimal degrees), longitude (LON, decimal degrees), altitude (ALT, in meters above mean sea level), period of the complete series and source of the data.

STATION	ALIAS	LAT(°N)	LON(°E)	ALT (m.a.s.l.)	PERIOD	SOURCE
ALBACETE	AB	39,0	−1,9	699	1905–2006	SDATS
ALICANTE	A	38,4	−0,5	82	1905–2006	SDATS
BADAJOZ	BA	38,9	−6,8	185	1905–2006	SDATS
BARCELONA	B	41,4	2,1	420	1905–2006	SDATS
BURGOS	BU	42,4	−3,6	881	1905–2006	SDATS
CADIZ	CA	36,5	−6,2	30	1905–2006	SDATS
CIUDAD REAL	CR	39,0	−3,9	627	1905–2006	SDATS
CORUNA	LC	43,4	−8,4	67	1905–2006	SDATS
GRANADA	GR	37,1	−3,6	685	1905–2006	SDATS
HUELVA	HV	37,3	−6,9	19	1905–2006	SDATS
HUESCA	H	42,1	−0,3	541	1905–2006	SDATS
LISBOA	L	38,7	−9,2	77	1905–2006	ECAD
MADRID	M	40,4	−3,7	679	1905–2006	SDATS
MALAGA	MA	36,7	−4,5	7	1905–2006	SDATS
MURCIA	MU	38,0	−1,1	57	1905–2006	SDATS
PERPIGNAN	PE	42,7	2,9	430	1905–2006	ECAD
SALAMANCA	SA	40,9	−5,5	790	1905–2006	SDATS
SEVILLA	SE	37,4	−5,9	31	1905–2006	SDATS
SORIA	SO	41,8	−2,5	1083	1905–2006	SDATS
TORTOSA	TO	40,8	0,5	50	1905–2006	SDATS
VALENCIA	V	39,5	−0,4	11	1905–2006	SDATS
VALLADOLID	VA	41,6	−4,8	691	1905–2006	SDATS
ZARAGOZA	Z	41,7	−1,0	245	1905–2006	SDATS
PAMPLONA	PA	42,8	−1,6	452	1922–2006	SDATS
SAN SEBASTiAN	SS	43,3	−2,0	252	1928–2006	SDATS
LEON	LE	42,6	−5,6	911	1938–2006	AEMET
BRAGANCA	BR	41,8	−6,7	690	1941–2006	ECAD
PORTO	P0	41,1	−8,6	93	1941–2006	ECAD
BILBAO	BI	43,3	−2,9	35	1947–2006	AEMET

data sources, including 86 land and island station series, marine data and daily gridded products from other sources. The spatial resolution of the grids is 5°. We made use of the complete available period 1850–2003, to obtain classifications of atmospheric circulation extended as far as possible into the past. Besides, the larger the statistical sample, the higher the confidence in the classification scheme. Circulation types (CTs) were therefore defined for the period 1850–2003 in terms of SLP for a domain centred in the Iberian Peninsula (grids were extracted for the area 30°N-50°N and 30°W-20°E) which includes 55 grid points. SLP Emulate data explain over 90% of the variability of SLP from ERA-40 (1959–2001) Reanalysis pressure data (ECMWF) in most of our domain, with a weaker reconstruction skill over Northern Africa.

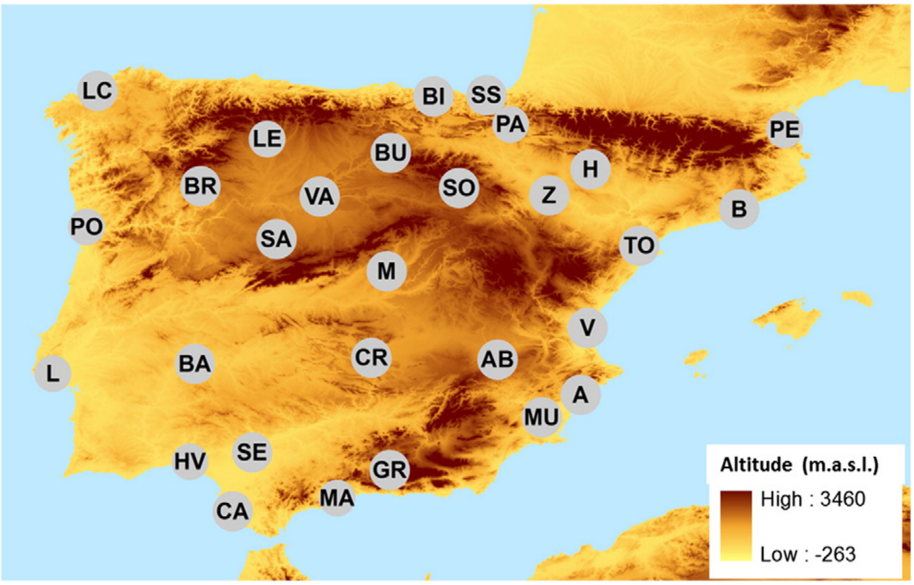

Fig 1. Station database, daily Tmax and Tmin series (see Table 1).

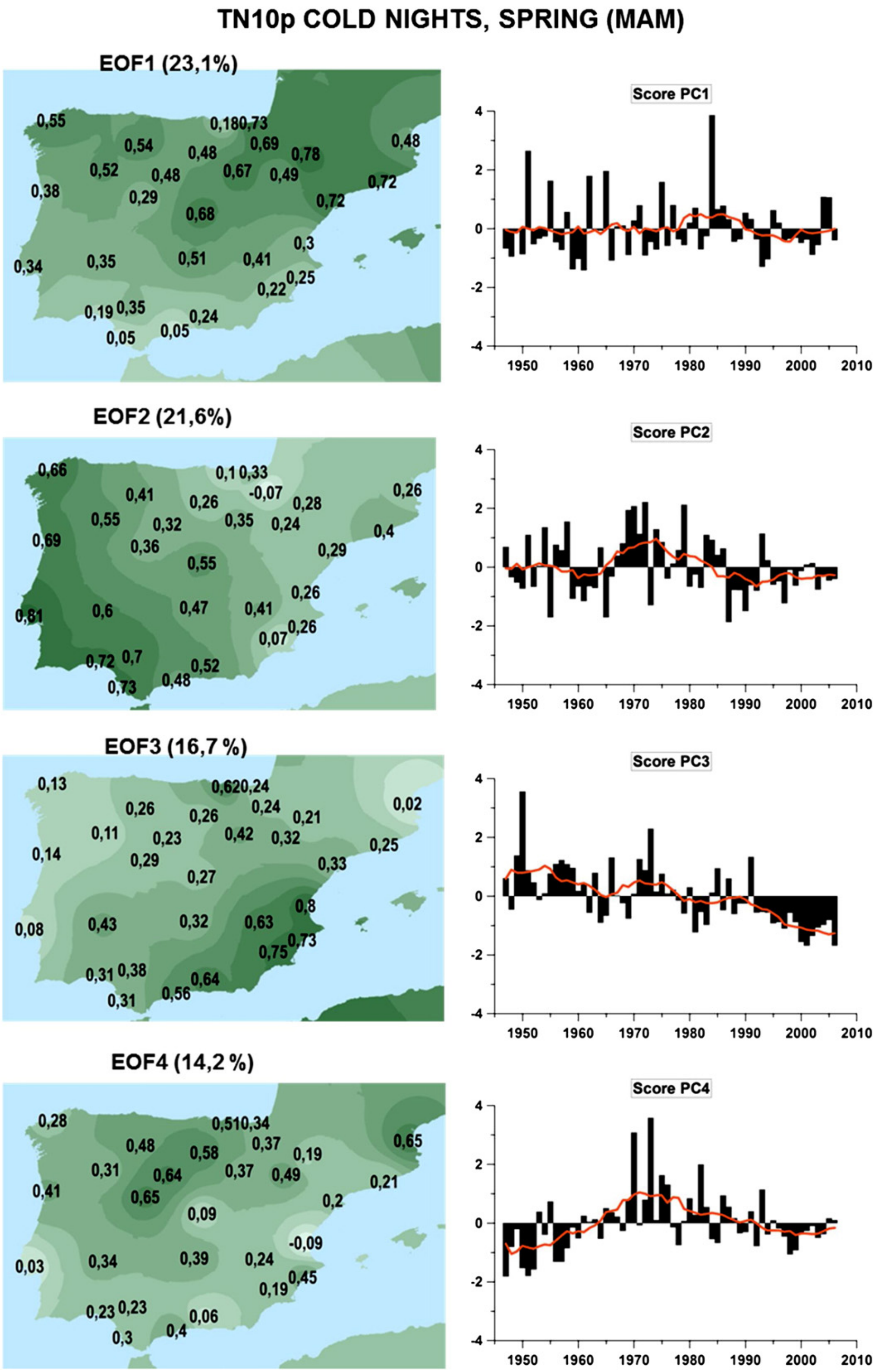

Fig. 2. Left panel: Loading factors at each station for each Empirical Orthogonal Function (EOF) derived from a rotated PCA in s-mode applied to the 29 TN10p series (cold nights) in 1947–2006 (explained variability in brackets). Right panel: Normalized time series of the PC scores (black bars) and 11-year moving averages (red line). For spring (MAM).

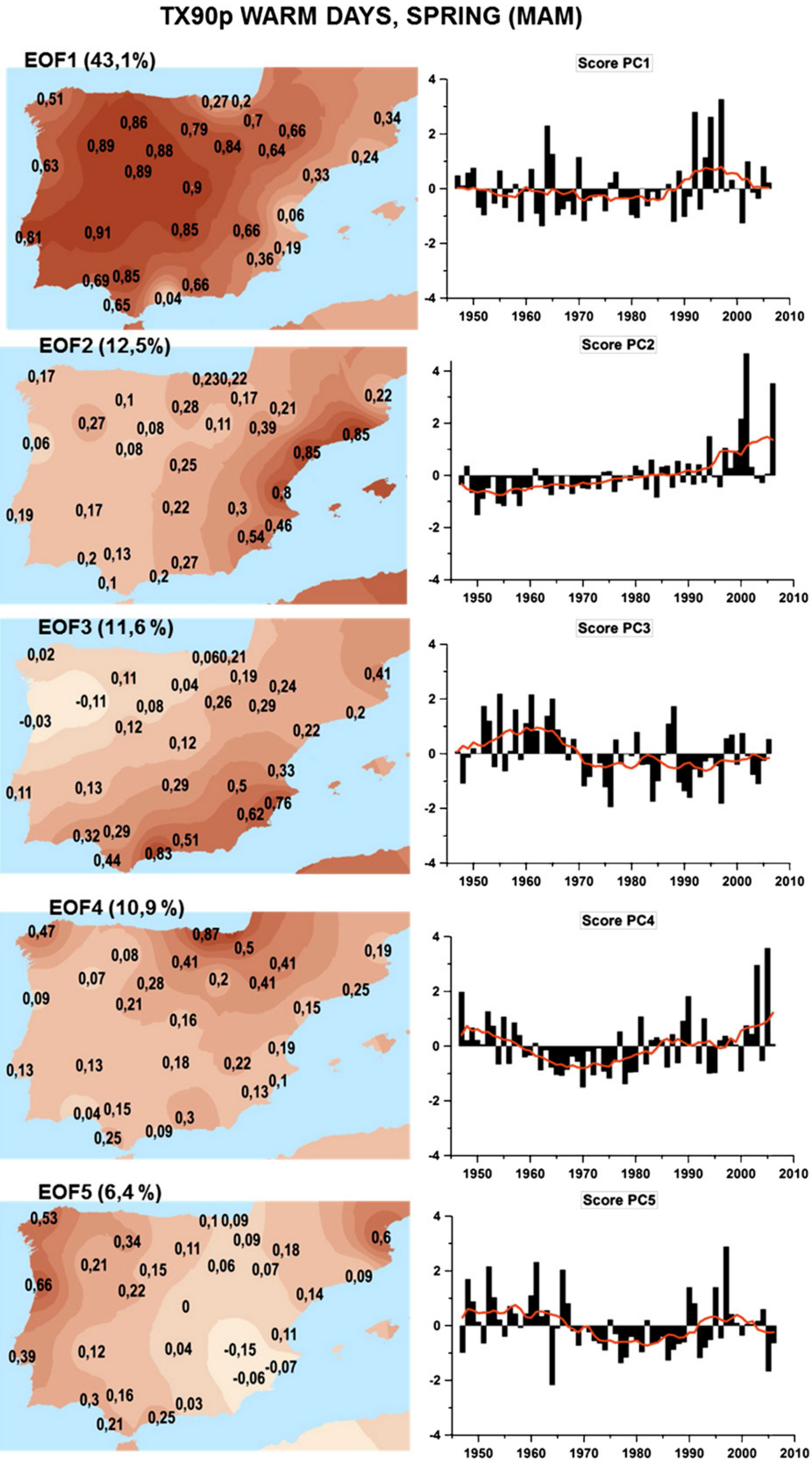

Fig. 3. As Fig 2 but applied to TX90p series (warm days) in 1947–2006 (explained variability in brackets). For spring (MAM).

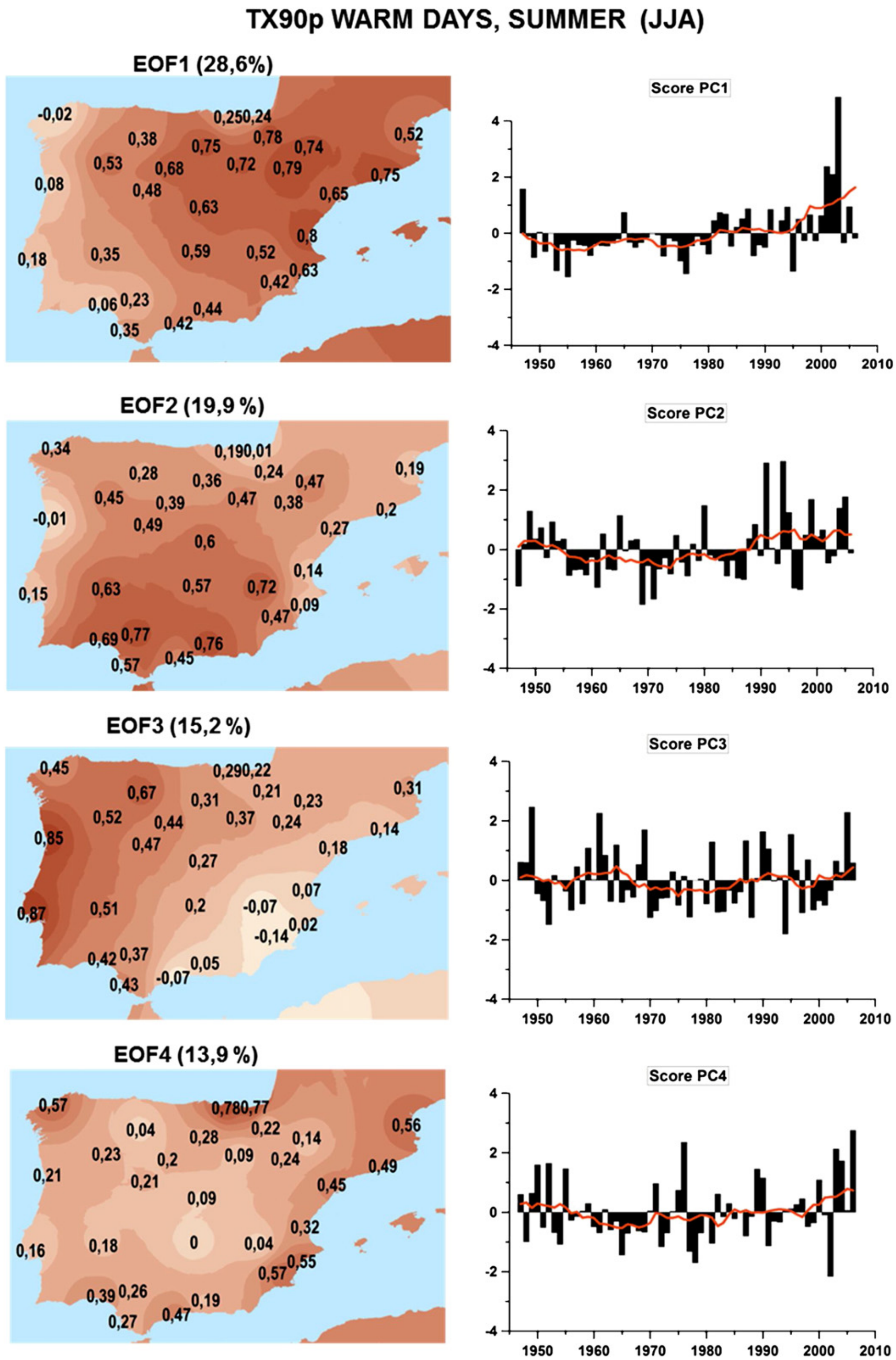

Fig. 4. As Fig 2 but applied to TX90p series (warm days) in 1947–2006 (explained variability in brackets). For summer (JJA).

Classifications (CTs) were obtained using a non-hierarchical Simulated Annealing and Diversified Randomization Clustering (SANDRA) method, described in detail by Philipp et al (2007). The algorithm is based on conventional k-means cluster analysis (CA) but differs in the ability to approximate the final classification to the global optimum. Non-hierarchical cluster

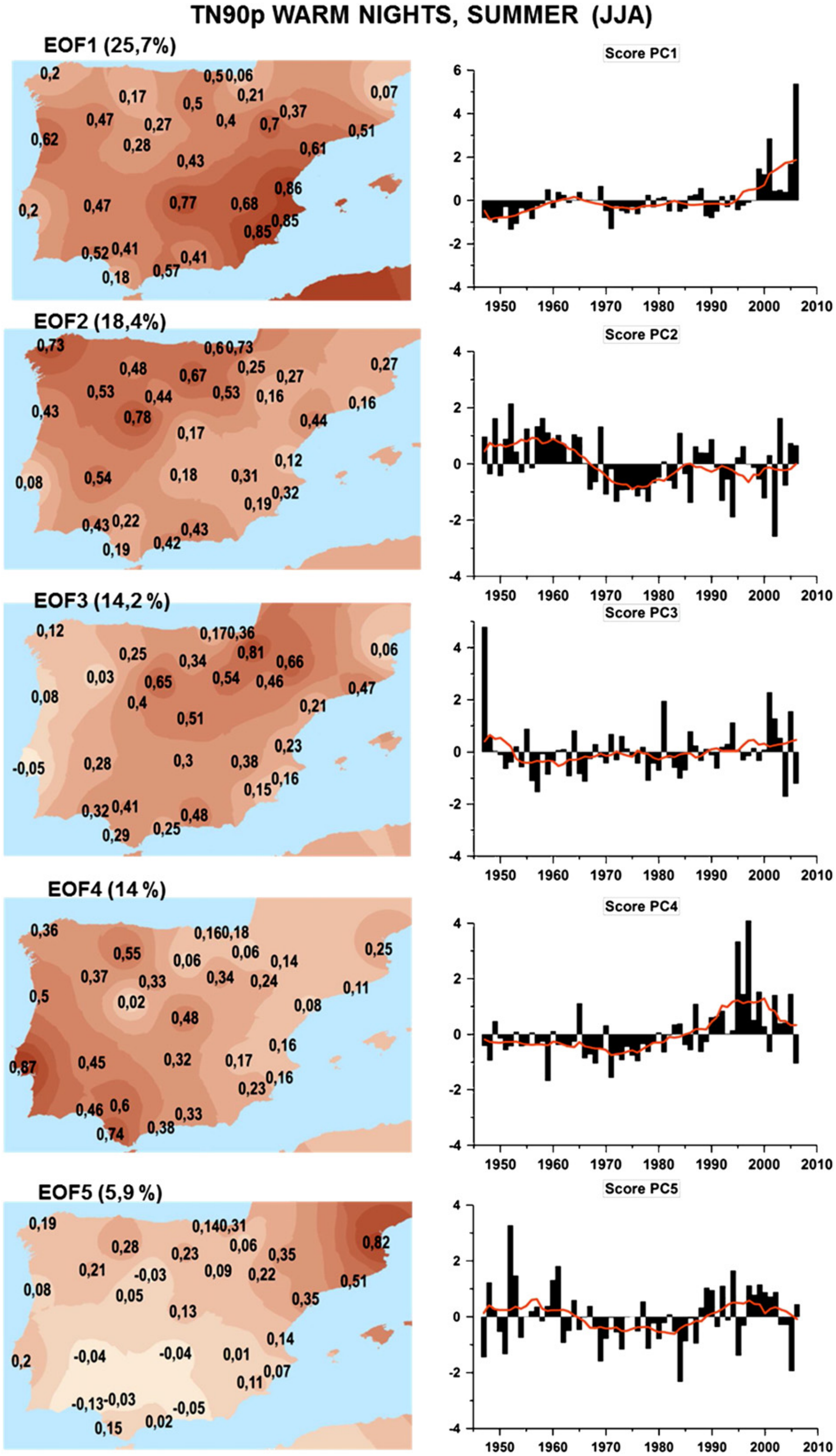

Fig. 5. As Fig 2 but applied to TN90p series (warm nights) in 1947–2006 (explained variability in brackets). For summer (JJA).

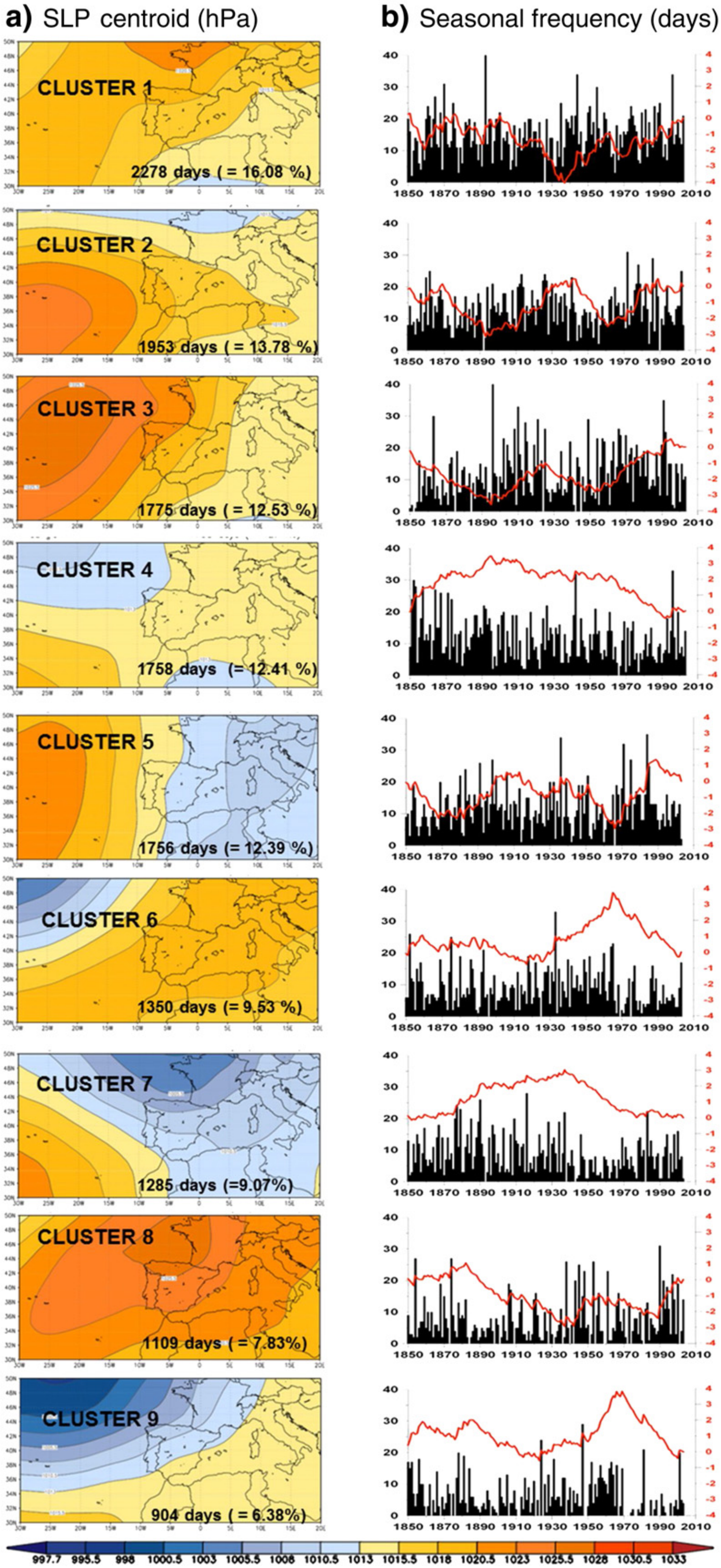
a) SLP centroid (hPa)
b) Seasonal frequency (days)
CLUSTER 1
2278 days (= 16.08 %)
CLUSTER 2
1953 days (= 13.78 %)
CLUSTER 3
1775 days (= 12.53 %)
CLUSTER 4
1758 days (= 12.41 %)
CLUSTER 5
1756 days (= 12.39 %)
CLUSTER 6
1350 days (= 9.53 %)
CLUSTER 7
1285 days (=9.07%)
CLUSTER 8
1109 days (= 7.83%)
CLUSTER 9
904 days (= 6.38%)
1850 1870 1890 1910 1930 1950 1970 1990 2010
997.7 995.5 998 1000.5 1003 1005.5 1008 1010.5 1013 1015.5 1018 1020.5 1023 1025.5 1028 1030.5 1033

analyses (such as k-means or SANDRA) require an a priori determination of the number of clusters. This decision was reached here by the *Dominance* criterion (Philipp et al., 2007): the same SLP grids are initially decomposed into principal components (PCs) using t-mode Varimax-Rotated Principal component Analysis (PCA) (Preisendorfer, 1988) and the number of independent PCs is taken as the number of clusters. The criterion provided 9 classes for spring (March to May, MAM) and 8 classes for summer (June to August, JJA).

A Mann–Kendall (M–K) non-parametric test (Kendall, 1938) was used to detect trends in the frequency of each CT, considering the whole period 1850–2003 and the sub periods 1950–2003 and 1970–2003. In case of significant trends for M–K test (p-value<0.05), a linear regression by least squares was performed, assessing trend-to-noise ratio tests to estimate its significance. Additionally, normalized series of cumulative anomalies of the temporal frequency were built (Philipp et al., 2007). They allow the identification of periods with predominant positive or negative anomalies of each CT frequency.

2.3. Sea surface temperatures and soil moisture anomalies

Additionally we have used information about well-known physical factors that influence summer and spring extreme temperatures (see Section 1):

Seasonal anomalies of East Atlantic SST from 1860 to 2010 have been built. Monthly SSTs (2.0 lat$\times$2.0 long) were acquired from the ERSST.v3 dataset (Extended Reconstruction Sea Surface Temperatures — Smith et al., 2008) and averaged for each 3-month season. We use East Atlantic domain as did Hertig and Jacobeit (2010) and Sousa et al. (2011).

Seasonal soil moisture information is taken in terms of percentage of Iberian area with very dry and very wet conditions, as proposed by van der Schrier et al. (2006), using the index scPDSI (self-calibrated Palmer Drought Severity Index- Wells et al., 2004; Sousa et al., 2011). The area considered for Iberia does not include the northern region (Sousa et al., 2011).

We will use a shorter period (1947–2000), shared by all variables (extreme series, CTs, SST and drought index) for the calculation of correlation coefficients (see Section 4.2).

2.4. Methods to relate temperature extremes to circulation types

1) To quantify which CTs are conducive to extreme temperatures (and with what effectiveness), the index EF (Jacobeit et al., 2009; Fernández-Montes et al., 2012) is defined for each CT and station. The period 1950–2003 (4968 days both for spring and summer), shared by all stations, is taken for this analysis. The index EF for a given CT and station is the ratio of percentage of extreme days at the station that take place under the CT (from total extreme days at the stations) to percentage of non-extreme days in the CT (from total non-extreme days at the station). When the index is significantly above 1, the CT is considered as conducive to extreme temperature at the station, since *the contribution of the CT to the total number of extremes is significantly higher than its contribution to non-extreme days*. The value of the index is computed at 1% of significance level by a Monte-Carlo resampling of 1000 series (each of them with 4968 days).
2) Once those CTs that are significantly conducive to extremes have been identified, a further step is to establish whether the contribution and the character of the CT for extremes are stable or not. Therefore, we analyse the temporal variations in the relationships between CTs and extreme temperatures (taking as long station series as possible, from 1905). As justified in Jacobeit et al. (2003) and Beck et al. (2007), the use of 31-year moving averages (m.a.) is appropriate for studying such low-frequency variations. Two indices are analysed: the *contribution of a CT* to the total number of extremes (extremes in the CT/ total extremes at the station) along with the *extreme potential or character of the CT* (extremes in the CT/total occurrence of the CT). A stable *extreme character* of the CTs would give confidence about the underlying dynamic causes of extreme temperatures. In contrast, a non-stable extreme character of the CTs could lead to the identification of other forcings influencing on decadal to multidecadal time scales.
3) To summarize changes of temperature within the CTs we assess trends in Tmax and Tmin (averaged from 23 station series in 1905–2003, Table 1) within all the 9 spring and 8 summer CTs.
4) Whereas patterns derived from a PCA permit the development of regression models (e.g., Fernández-Montes and Rodrigo, 2011), the CTs derived from a cluster analysis are not orthogonal and indicate dependence between them (not shown). Thus, for an estimation of the relationship between interannual oscillations in the frequency of extremes and in the CTs frequency (as well as to anomalies of SSTs and percentage of dry/wet area, see Section 2.3) a simple Spearman rank correlation test is applied.

3. Results

3.1. Changes in extreme temperature indices (1947–2006)

To describe the fluctuations of cold nights and warm days (warm nights and days) for spring (summer) and to identify homogenous regions and change points we perform a rotated PCA on s-mode (Preisendorfer, 1988), as did Brunet et al. (2007) in the regionalization of seasonal Tmax, Tmin and annual extreme indices. For each of the four indices, the 29 station extreme series from 1947 to 2006 are reduced into empirical orthogonal functions (EOFs) which score series represent the evolution of the variables (time-plot) for the corresponding region (identified by high loading factors at the stations in the maps) (Figs. 2–5).

In the following, we describe these changes in the seasonal frequency of extreme temperatures. Later we will search for correlations between these regional time series and CTs frequency (in Section 3.3).

According to Fig. 2, in spring the frequency of cold nights (TN10p) do not show pronounced changes for the first principal component (EOF1, representing NE region with the lowest

Fig. 6. a) Centroids patterns of the SLP clusters (hPa, scale in the bottom) or CTs for spring (MAM) season; b) Seasonal frequencies (days) of the clusters are shown (bar charts, left axis) as well as normalized cumulative anomalies of the frequency (red, right axis).

loading factors towards South Iberia). EOF2 (representing W/SW region) and EOF4 (Central North) exhibit increasing occurrence of cold nights until the mid-1970s and a decrease thereafter. By contrast, cold nights decrease throughout the whole period for EOF3 (representing SE region, but also loaded heavily onto BI station). The decrease appear more striking from the mid-1970s onwards. This is coherent with Brunet et al. (2007) who obtained increase in spring Tmin in 1973–2005, more pronounced for SE regional series.

Fig. 3 shows the PCA applied to spring warm days (TX90p). Increases are identified in the late 1980s to early 2000s for EOF1, which identifies central and westernmost Iberia (all stations with loading factors between 0.6 and 0.9) and accounts for a 43% of total variability in the index. The second principal component, EOF2, identifies the East-Mediterranean region, which shows increases in warm days throughout the whole period (with high occurrence in the 2000s). The EOF3, representing central South region, exhibits a great frequency of warm days in the 1950s and 1960s, and less frequency in the next 3 decades. EOF4 is loaded towards northeast Cantabrian stations and shows a decrease in warm days from 1947 to mid-1970s and increase thereafter. EOF5 present the highest loadings at Atlantic stations such as LC and PO; also PE station present a high loading which is explained by the important Atlantic influence on this station (Fig. 1). Time score series of EOF5 exhibits (as EOF3 does) higher TX90p frequency in the 1950s-1960s and (as EOF1) in the 1990s with negative anomalies in between.

Regional patterns of summer warm days (TX90p) are shown in Fig. 4. The EOF1, which accounts for 28.6 % of the total variability, identifies the NE/E region and shows a clear uptrend in warm days from mid 1970s, more remarkable in the last decade. EOF2 (central-southern region) and EOF4 (stations in the Mediterranean and Cantabrian coasts) also show increases in the 1980s onwards. EOF3 identifies Atlantic and westernmost region and exhibits the highest interannual variability without pronounced changes (but a slightly lower frequency of warm days from around 1970 to 1980).

According to Fig. 5, the frequency of warm nights (TN90p) in summer exhibits a clear increase in the 1990s for the EOF1, with the highest loadings over easternmost Iberia, but also notably influence by other stations (e.g., PO). Meanwhile for EOF4, with high loading factors identifying a SW/W region, an equivalent change occurs earlier (around mid-1980s). For EOF2 (NW region) warm nights were more frequent in the 1950s and 1960s, and less frequent in the 1970s and 1980s. A similar (but smoother) behaviour is observed for EOF5 (representing north-easternmost stations, i.e., B and PE), with peaks of warm nights frequency observed in the 1950s and 1990s to 2000s. Finally, EOF3, loaded towards NE inland and high altitude stations, do not exhibit any pronounced changes in warm nights.

3.2. Circulation types: brief description, variability and trends

We have classified daily SLP grids from 1850 to 2003, including a total of 14,168 days (×55 grid points) for each 3-month season. Fig. 6a (Fig. 7a) shows the derived 9 (8) SLP centroids derived from the cluster method for spring (summer): in the SLP scale, in hPa, the highest values are in red/orange and the lowest in blue colours. Figs. 6b and 7b display the temporal frequency (days) of the CTs in each year (black bar-charts, left axis) in 1850–2003. The normalized series of cumulative anomalies of the frequency are shown in red. The presence of trends in the frequency for the whole period was tested by means of M–K and trend-to-noise tests (Tables 2, 3).

3.2.1. Spring

Fig. 6a shows the derived CTs for spring. In CT1 and CT8, high pressure is observed over Western France and Northern Iberian Peninsula, with prevailing easterly winds over Iberia. Northerly types are CT3, with extended Azores Anticyclone in the North-Atlantic (NA) and CT5, with a steep gradient between the Azores High and low pressure in the Mediterranean. More westerly zonal circulations occur in CT9 (W-SW flow, Icelandic low shifted to south), CT6 (SW flow over NW Iberia) and CT7 (low pressure over Western France, with prevailing NW flow). CT2 is characterized by a slight south-shift of the Azores High, with NW flow over North Iberia. Finally CT4 depicts a weak Azores High and NA low pressure; hence a NW stream over North-western Africa favours cyclogenesis in the lee of Atlas Mountain (Sahara low) which is frequent in spring (Trigo et al, 1999).

For 1850–2003, the M–K test detected significant (p-value <0.05) negative trends in the frequency of clusters 4, 7, and 9 (westerly types), and a positive trend for cluster 3 (North Atlantic Anticyclone). Trends for the shorter period 1950–2003 are also significant in a few cases: a positive trend in CT7 and negative trend in CT9. From 1970 to 2003, significant down-trends (uptrends) are found for CT5 (CT9).

3.2.2. Summer

In summer (Fig. 7a), Azores High is observed in all the SLP centroids, though with different intensity and extension: An anticyclone bridge is observed in CT1, the anticyclone is more intense in CT5, CT7 and CT2 and it is more extended to West France in CT4, 5 and 6. CT3 and CT8 depict a low pressure, respectively to Northern France and East Atlantic. A thermal low is observed in Northern Africa in all the CTs. The relative low pressure in South/East Spain in the CTs 4 and 7 is also very likely linked to heat troughs development.

The Mann–Kendall test (Table 3) detected significant (p-value<0.05) negative trends over 1850–2003 in CTs 1, 6, and 8, and positive trends for CT 5 and 7. The most pronounced positive trend is detected for CT5 (deep Azores anticyclone extended to West France) and negative trend in cluster 8 (low pressure in NA). It is worthy highlighting the increasing frequencies of the thermal low-related CTs: CT4 (1950–2003), and CT7 (in 1910s onwards, Fig 7b). Finally, over 1970–2003, a significant positive trend in CT8 frequency was detected. During the hot summer of 2003 (the last year in our classification), the most frequent types were CT1 (25 days), CT2 (19 days), CT4 (16), and CT8 (12).

In general, a high inter-annual variability of CTs frequency is observed in both seasons (Fig 6b, Fig 7b). Thus, Tables 2 and 3 show the great sensitivity of the trends to the period analysed (1850–2003, 1950–2003, 1970–2003) and none of the CTs shows any significant linear uninterrupted trend.

3.3. Spatiotemporal links between circulation types and extreme temperature indices

In this section the incidence (in any) of the distinct CTs on the local occurrence of moderate extreme temperature days/

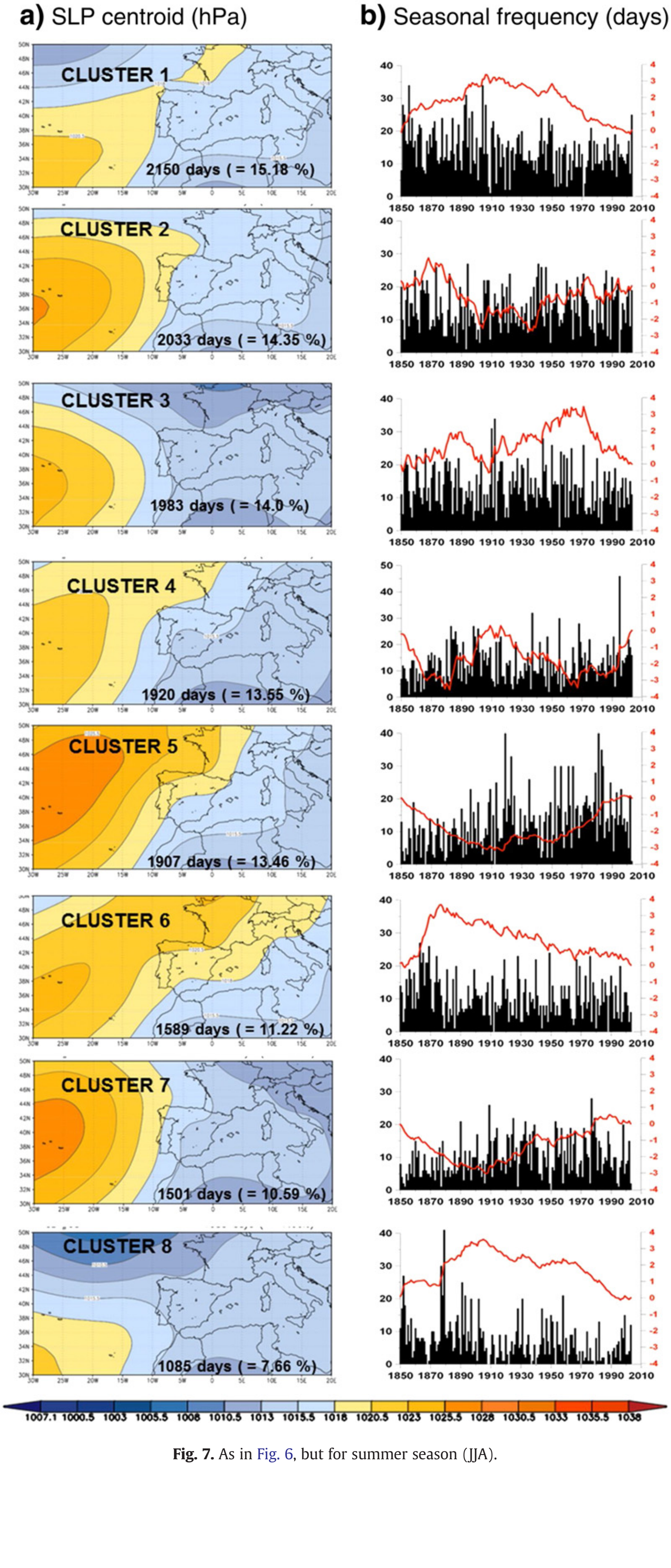

Fig. 7. As in Fig. 6, but for summer season (JJA).

Table 2
Trends in the frequency of spring (MAM) SLP-Clusters in 1850–2003 and more recent sub periods. Statistic of Mann–Kendall is shown in bold when trends are significant (p-value<0.05). Linear trend (days) refers to the magnitude in the whole period (154, 54, and 34 y respectively) and T/noise is the quotient between linear trend and standard deviation. Linear trends do not reach the 5% of significance level in any case (no T/noise above 1.96).

Spring Cluster (CT)	1850–2003				1950–2003				1970–2003			
	Z(M-K)	p-value	trend	t/noise	Z(M-K)	p-value	trend	t/noise	Z(M-K)	p-value	trend	t/noise
1	1.46	0.144	2.32	0.35	−0.23	0.822	−0.32	−0.05	−0.24	0.809	−0.07	−0.01
2	1.24	0.215	2.18	0.36	1.36	0.183	3.87	0.59	−0.83	0.405	−4.51	−0.61
3	**3.18**	**0.001**	6.08	0.76	−0.58	0.565	−1.17	−0.16	−1.83	0.068	−6.24	−0.84
4	**−2.95**	**0.003**	−6.08	−0.89	−0.03	0.976	0.54	0.09	1.54	0.125	5.70	0.90
5	0.48	0.631	1.41	0.21	0.48	0.646	1.32	0.18	**−2.49**	**0.013**	−10.5	−1.43
6	−1.06	0.291	−1.74	−0.30	−1.72	0.093	−5.80	−1.01	1.44	0.149	2.66	0.59
7	**−2.30**	**0.021**	−4.22	−0.70	**2.14**	**0.039**	4.53	0.95	0.15	0.878	0.30	0.06
8	0.59	0.554	2.40	0.35	1.77	0.085	5.16	0.69	1.76	0.078	8.00	1.09
9	**−2.04**	**0.041**	−2.34	−0.39	**−2.45**	**0.019**	−8.13	−1.33	**2.70**	**0.007**	4.67	0.95

nights is shown by means of the index EF (see methods Section 2.4). In the maps (Figs. 8a, 9a, 10a, 11a) the value of the index has been interpolated (from the 29 stations) using a simple algorithm with the inverse of the squared distance. Naturally, only values at the stations are strictly valid. A black line delimits the stations with index EF above 1, i.e., stations with higher fraction of extreme days than of non-extreme days due to the given CT (at 1% s.l.).

Additionally, to quantify the relationship between interannual changes in extreme temperatures (EOFs regional extreme series, Section 3.1, Figs. 2–5) and seasonal CTs frequency, correlation coefficients are presented in Table 4a–b. We also indicate in this Table 4 the correlation coefficients between extreme temperature series and East Atlantic SST and drought index (Section 2.3), but they will be discussed in Section 4. To calculate the correlations, a period common to all the mentioned variables was taken (1947–2000).

3.3.1. Spring CTs and cold nights/warm days

Fig. 8a displays the index EF for the CTs (SLP clusters in Fig. 6a) that are involved in the local occurrence of cold nights (TN10p) in spring. We observe the most widespread incidence of CT3 and CT5, i.e., the most northerly types. Fig. 9a shows the incidence of the clusters on warm days (TX90p), being CT6 and CT8 the most important for mainland Iberia.

In CT1 mostly clear sky conditions and cold advection from the NE favour low minimum temperatures in the Northeast quadrant of Iberia (only statistically significant at BI and V, Fig 8a). In contrast, over SW Iberia the easterly flow (from land) produce warmer than normal conditions, hence a negative correlation (rho = −0.34, Table 4a) exists between CT1 and cold nights/EOF 2 (Fig 2). During day time, similarly, the easterly advection favours warm days over western stations (Fig 9a) and the high pressure in France promotes high insolation and calm winds in Northernmost Iberia. The prevailing E/NE component of flow (from the Mediterranean Sea) causes moderate maximum temperatures in the East.

CT2 is connected to warm days in the SE/Mediterranean region (Fig 9a), because the Azores High is quite extended over West Iberia, involving a well-established northwest inland flow over these areas. In contrast, cool conditions are expected in the North and West Iberia, as indeed supported by the negative correlations (Table 4a, EOF4 and EOF5-Fig 3).

CT3 is characterised by northerly circulation due to an extended and intense Azores High and lower pressure towards the Mediterranean Sea. It causes cold nights over mainland Iberia (Fig 8a) except for some Atlantic and Ebro Valley stations. Concordantly, a significant positive correlation (rho = 0.28) is found between cold nights in the SE region (EOF3, Fig. 2) and the frequency of this CT (Table 4a).

CT5 centroid pattern indicates strong northerly advection (i.e., of Artic air masses), given the steep pressure gradient between the Azores High and low pressure in the Mediterranean. Hence cold conditions are generalized for this CT, with a strongest link at NW and NE stations. Thus, regional series of cold nights representing North region (see EOF1 in Fig. 2) are positively correlated (rho = 0.40) with the frequency of this CT (Table 4a).

The SW flow in CT6 introduces warm air from lower latitudes, linked to warm days for a large number of stations (index EF > 1, Fig. 9a). The greatest incidence is on Northern

Table 3
As in Table 2, but for summer (JJA) season.

Summer Cluster (CT)	1850–2003				1950–2003				1970–2003			
	Z(M-K)	p-value	trend	t/noise	Z(M-K)	p-value	trend	t/noise	Z(M-K)	p-value	trend	t/noise
1	**−3.25**	**0.001**	−6.19	−0.98	1.66	0.104	4.11	0.80	1.21	0.228	4.38	0.88
2	0.90	0.370	1.09	0.18	0.14	0.887	−0.37	−0.06	−0.08	0.939	−0.40	−0.06
3	−1.07	0.286	−1.99	−0.32	−0.94	0.354	−4.19	−0.66	1.13	0.257	1.46	0.26
4	1.85	0.064	3.47	0.51	**2.94**	**0.004**	7.87	1.06	1.72	0.085	6.88	0.95
5	**5.20**	**0.000**	10.43	1.33	−0.42	0.681	−1.83	−0.22	−1.93	0.054	−8.9	−1.06
6	**−2.29**	**0.22**	−4.11	−0.70	−0.19	0.852	−0.57	−0.10	−0.42	0.672	−2.03	−0.37
7	**2.97**	**0.003**	4.40	0.78	−0.93	0.362	−2.37	−0.37	−1.86	0.063	−6.44	−1.02
8	**−4.34**	**0.000**	−7.08	−1.12	−0.74	0.476	−2.64	−0.55	**2.46**	**0.14**	5.06	1.23

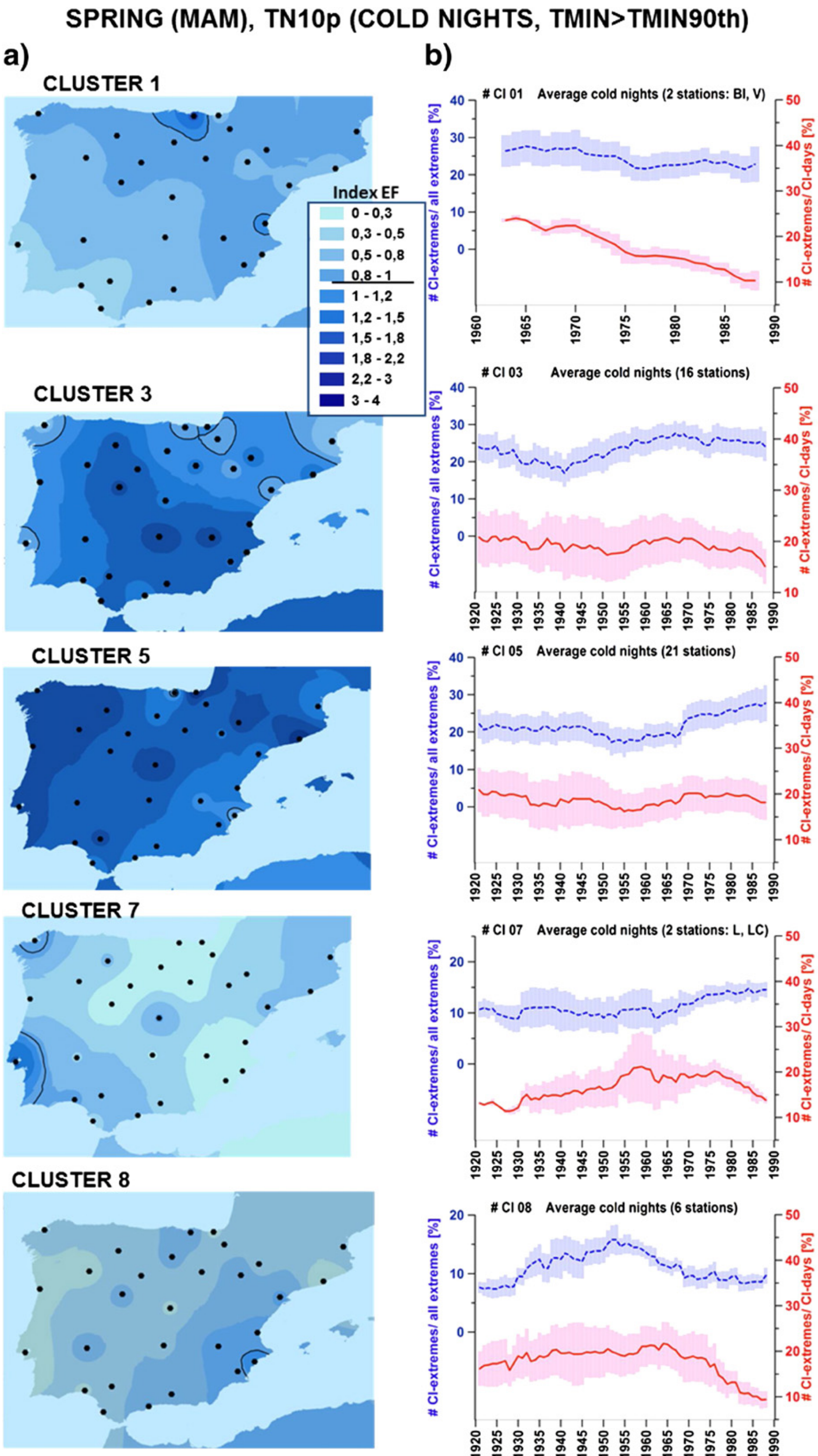

Fig. 8. a) Index EF (see legend in first map and definition in method section) for spring clusters (Cl) or CTs significantly conducive to the occurrence of cold nights (Tmin<Tmin10th). b) The percentage of extreme days within-type respect to the overall frequency of the CT is plotted (in red, right axis, named *extreme potential or extreme character of the CT* in the text) alongside the percentage of extreme days within the CT with respect to total observed extremes (in blue, left axis, named *contribution of the CT*).

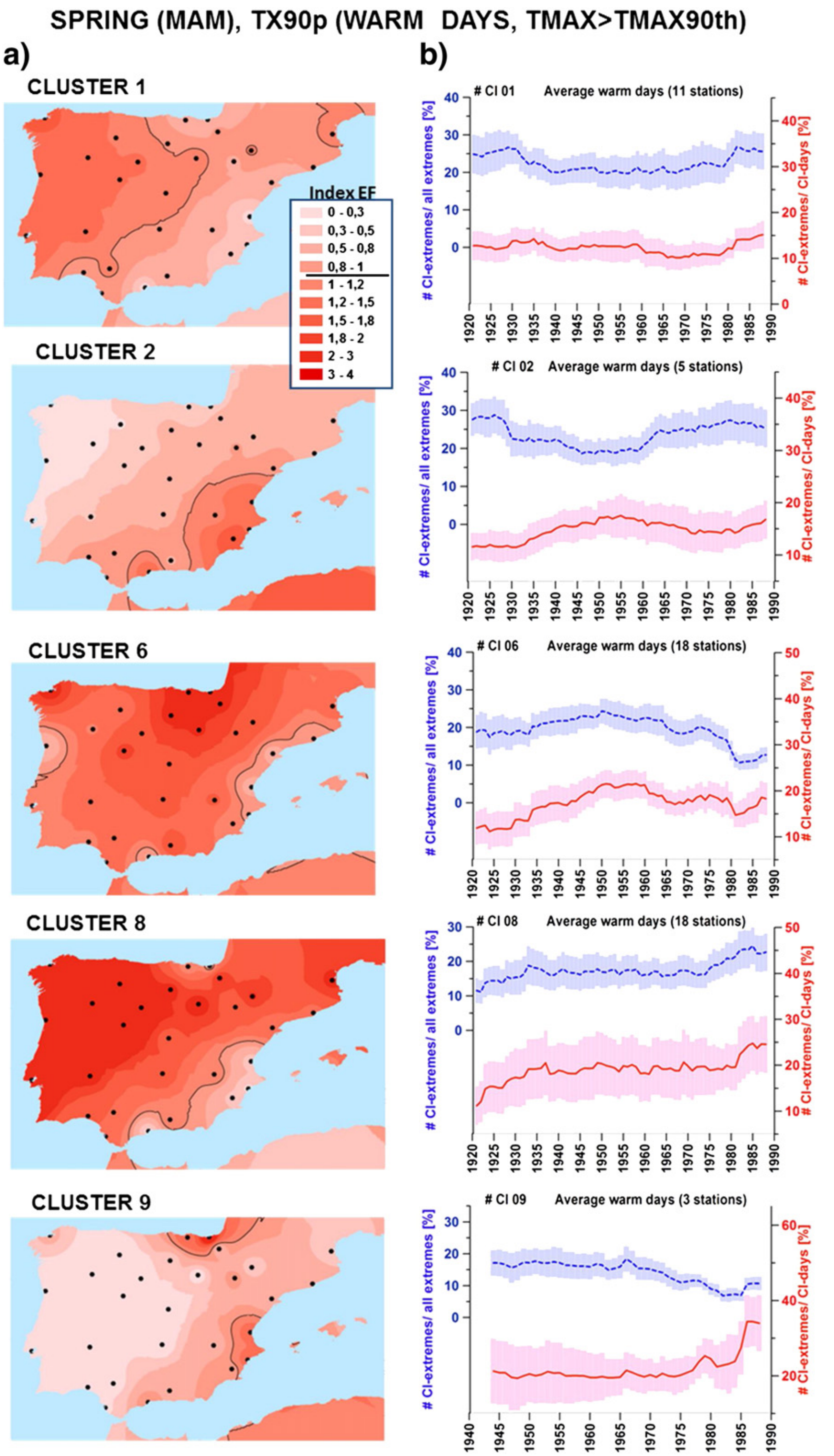

Fig. 9. As in Fig. 8, but for spring occurrence of warm days.

stations, linked to the downslope effect (Rasilla et al., 2010) and warming of the air throughout Iberian Plateau. Hence there are positive correlations between this CT and warm days in Central/NW Iberia (EOF1, Fig. 3), South (EOF3) and North (EOF4) and negative with Mediterranean region (EOF2) (Table 4a).

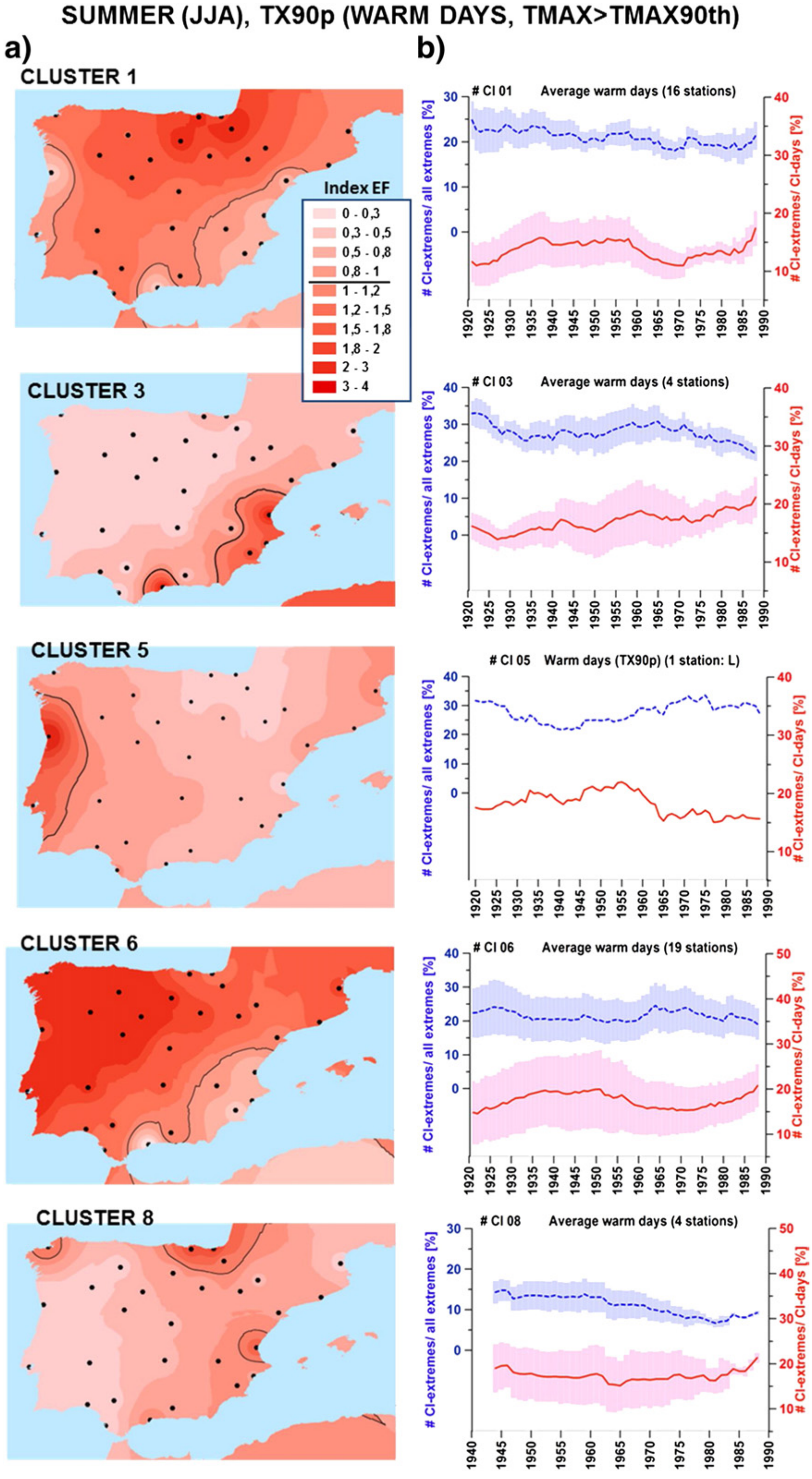

Fig. 10. As in Fig. 9 and Fig. 8, but for summer occurrence of warm days.

CT7 depicts a pressure gradient between southern displaced Azores Anticyclone and low pressure system in North Iberia/Western France, yielding NW flow. Hence Atlantic locations (LC, L), exposed to stronger NW winds, are prone to cold nights under this CT (Fig. 8a). Consistently, temporal changes in cold nights for West Iberia (EOF2 in Fig. 2) are correlated with the frequency of this CT (Table 4a). The incidence of CT7 on warm days is limited to Mediterranean

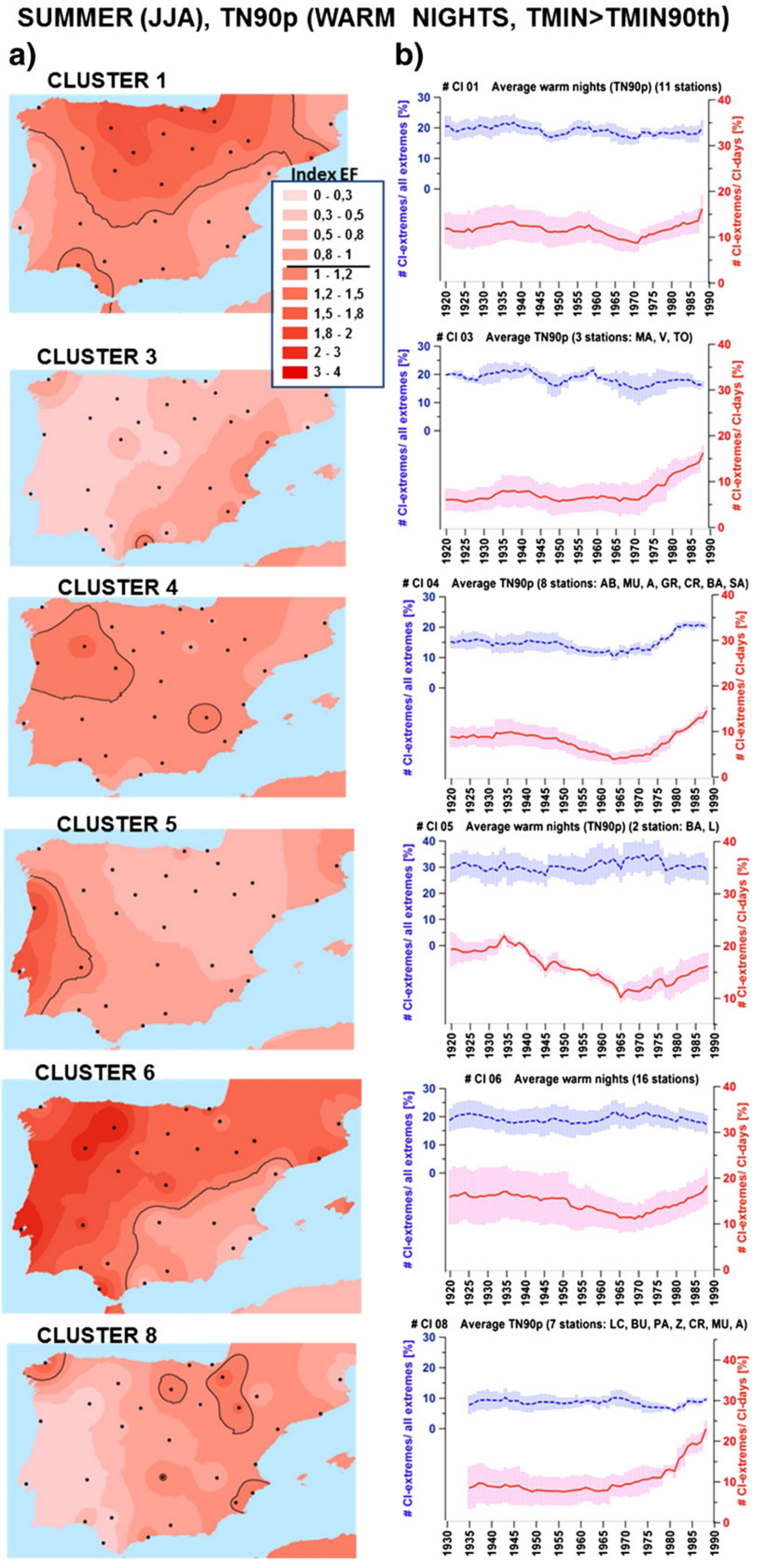

Fig. 11. As in Fig. 8, but for summer occurrence of warm nights.

Table 4
Correlation coefficients (period 1947–2000) between normalized regional extreme series (rows, from Section 3.1) and anomalies of CTs frequency (Section 3.2), EA SST and soil moisture conditions (Section 2.3). Values in bold are significant at 5% level (p-value<0.05) and * marked values significant at 10% level (p-value<0.1). Correlation coefficients at p-value>0.1 are not shown, a) for spring (MAM) and b) for summer (JJA) CN = Cold Nights, WD= Warm days, WN= Warm Nights.

a

Spring	CT1	CT2	CT3	CT4	CT5	CT6	CT7	CT8	CT9	EA_SST	%Dry Area
TN10p EOF1					**0.40**					**−0.38**	
TN10p EOF2	**−0.34**					**−0.34**	**0.36**				
TN10p EOF3		**−0.29**	**0.28**			0.24*	**−0.39**				
TN10p EOF4		**0.33**							**−0.32**		
TX90p EOF1						**0.30**		**0.40**	**−0.31**		**0.32**
TX90p EOF2						**−0.35**	**0.38**	**0.35**	−0.25*	0.25*	
TX90p EOF3					−0.26*	**0.37**			**0.52**	**0.41**	
TX90p EOF4		**−0.41**	**−0.31**	0.26*	−0.26*	**0.29**					
TX90p EOF5		**−0.29**					**−0.49**	0.23*		**0.28**	

b

Summer	CT1	CT2	CT3	CT4	CT5	CT6	CT7	CT8	EA_SST	%Dry Area	%Wet Area
TN90p EOF1											
TN90p EOF2		**−0.29**									
TN90p EOF3			−0.24*				−0.23*				
TN90p EOF4			−0.23*						**0.46**	**0.38**	
TN90p EOF5		**0.27**							0.27*		
TX90p EOF1											
TX90p EOF2	**0.31**				0.24*					**0.36**	**−0.31**
TX90p EOF3		**−0.32**	**−0.41**			**0.39**					
TX90p EOF4							**−0.49**				

region (with a positive correlation, WD_EOF2), although only significant at MA according to the index EF (not shown).

CT8. The anticyclone extended over the Iberian Peninsula is related to clear sky conditions (and mostly calm winds) which favour high daytime temperatures and cooling during the night. In East Iberia the easterly flow creates cooler-than-normal conditions, significant at Alicante (A) station (Fig. 8a). For other 5 stations (MA, MU, A, V, TO), index EF is between 0.8 and 1 (5 stations considered for temporal plot in Fig. 8b). CT8 is conducive to moderate warm days in the IP (with the exception of SE Mediterranean region, Fig. 9a) since the Anticyclone blocks westerly and northerly flows and allows easterly circulation. Hence there is a positive correlation between CT8 frequency and regional series, especially for Central-West region (Table 4a, EOF1 in Fig. 3).

CT9 gives rise to warm days in the SE and East Cantabrian Coast (Fig. 9a). This is due to warm (and initially moist) SW winds which favour warming (Föhn effect) downslope mountain chains. Besides, to the SE quadrant the southerly advection can be especially warm and dry if the air comes from Africa. Indeed, a high correlation (rho = 0.51) is found between CT9 frequency and regional warm days series representing South Mediterranean region (Table 4, EOF3 in Fig. 3).

Fig. 8b shows the temporal variations of the extreme (cold) behaviour of CT1, CT3, CT5, CT7 and CT8. The plotted lines are the average series over the longest stations-series (1905–2003) affected by each cluster, and STD of the series is shown by moving bars. The contribution to the total number of extremes (discontinuous blue line, left axis) is plotted alongside the extreme potential or character of the CT (solid red line, right axis), using 31-year m.a. (therefore, covering the period 1920–1988). Except for northerly flow (CT5), the remaining CTs exhibit a drop in their cold character around 1970 onwards. Within-type changes in warm days (Fig. 9b) indicated slight variations in most types, with a generalized increase in the last decade of 1980s. The causes of these changes will be discussed in Section 4.

3.3.2. Summer CTs and warm days/ warm nights

Focusing on the index EF that links summer circulation types to the occurrence of warm days (maps in Fig. 10a) and warm nights (Fig. 11a):

In CT1, the Azores High and an anticyclone bridge in West Europe inhibits the entry of air from the North Atlantic to North Iberia. This situation is conducive to high temperatures especially in northern and continental areas of Iberia (Figs. 10a–11a). The less affected areas are Central Atlantic and Mediterranean coasts where sea breezes prevail over inland weak fluxes. In the period 1947–2003, warm days' time series for central-south region (EOF2 in Fig. 4) and the frequency of CT1 positively correlates (Table 4b).

In CT6 the Azores anticyclone is deeper and extends with a ridge further towards Western Europe, blocking the displacement of air from the Atlantic and, in contrast, favouring easterly circulation. This gives rise to warm (day and night time) conditions in most of the IP, especially to the NW (as supported by values of indexEF > 2, Figs. 10a, 11a). Hence regional EOF3 series (representing west stations, Fig. 4) are positively correlated with CT6 frequency (Table 4b). At continental stations which do not reach so high index EF values for warm days (e.g., CR, GR) in both CT1 and CT6, warm nights occurrence becomes non-significant, due to radiative losses during the night.

In CT5, as in CT6, flow from E/NE arrives to Iberia, but Azores High is more intense and extended, providing stronger easterlies. Hence, the advection is cooler (than CT6) for north-easternmost stations but connected to warm conditions

Table 5
Trends in average Tmax and Tmin within the CTs for the period 1905–2003 and two sub-periods a) For spring (MAM) and b) for summer (JJA). Mann–Kendall derived trends significant at 5% level (p-value <0.05) are in bold; only sign of the trend is shown if 0.05<p-value<0.5; null trends (p-value>0.5) are indicated by "0". Slopes of the trends (in °C/decade) are shown when linear fit is significant (t-test at 5% level).

	Total period 1905–2003		First half 1905–1953		Second half 1954–2003	
	Tmax	Tmin	Tmax	Tmin	Tmax	Tmin
a) Spring						
CT1	+	+	0	0	+	**0.47 (±0.17)**
CT2	**0.17 (±0.07)**	+	+	+	0	0
CT3	**0.20 (±0.08)**	+	**0.78 (±0.26)**	+	0	0
CT4	+	+	0	0	+	**0.54 (±0.22)**
CT5	0	0	+	**0.37 (±0.18)**	+	+
CT6	+	+	0	0	**0.70 (±0.29)**	+
CT7	+	+	+	0	0	−
CT8	**+**	+	0	0	+	+
CT9	**0.29 (±0.09)**	**0.21 (±0.05)**	+	0	**0.70 (±0.22)**	**0.61 (±0.16)**
	1905–2003		1905–1953		1954–2003	
	Tmax	Tmin	Tmax	Tmin	Tmax	Tmin
b) Summer						
CT1	**0.20 (±0.06)**	**+**	+	0	**0.52 (±0.13)**	**0.41 (±0.09)**
CT2	**0.17 (±0.04)**	+	**0.32 (±0.14)**	0	**0.39 (±0.11)**	**0.41 (±0.09)**
CT3	+	0	**0.35 (±0.17)**	0	+	+
CT4	**0.14 (±0.05)**	**0.10 (±0.04)**	**0.45 (±0.16)**	0	**0.47 (±0.14)**	**0.50 (±0.11)**
CT5	**0.13 (±0.05)**	**0.10 (±0.04)**	**0.42 (±0.13)**	**0.23 (±0.10)**	0	+
CT6	**0.16 (±0.06**	+	+	0	**0.46 (±0.19)**	**0.42 (±0.14)**
CT7	**0.15 (±0.07)**	+	**0.50 (±0.14)**	**+**	0	+
CT8	**0.43 (±0.10)**	+	+	0	**0.58 (±0.23)**	**0.58 (±0.16)**

Trends in °C/decade.

in Westernmost Iberian stations (Figs. 10a, 11a), since easterly circulation from inland is much stronger than Atlantic breeze.

CT3, by contrast, favours the entrance of air masses from the North (due to the pressure gradient between Azores and France), permitting cool or temperate summer temperatures in mainland IP. However, the NW flow gives rise to warmer than normal conditions to the SE quadrant (V, MA, MU, A) (Figs. 10a, 11a) where masses of air arrive warmer, having travelled over the Iberian Peninsula. For warm nights the highest incidence is at MA station (Fig 11a), i.e., probably because sea breeze weakens during the night and land breeze reinforce this northerly wind (known as *Terral* wind in Malaga).

In CT4, the heat low extended from Northern Africa to the Southern half of Iberia and a weak subsidence of air (weak Azores anticyclone) enables convection and formation of clouds that permit relatively high nigh-time temperatures. Most stations have an index EF between 0.8 and 1.5. The most affected stations are those to the NW and to the SE. Indeed, the highest average Tmin for the whole IP is obtained under this CT (not shown).The possible presence of clouds could explain why the incidence on day-time temperatures does not arise.

CT8 depicts Icelandic low shift to the south and westerly flow over the West Iberian façade. This pattern has a warm influence over SE coast (Figs. 10a, 11b) although less than the NW flow (CT3). Under this configuration the Cantabrian Coast and Ebro Valley are also affected because of the SW flow (downslope heating mechanism) (Figs. 10a, 11b). Besides, the low pressure in the East Atlantic in CT8 provides westerly instable flow with the probability of cloud development to the North of Iberia.

Fig. 10b represents the within-type variations in warm days (1920–1988), with mostly increases (red lines) in the 1930s to 1960s and the 1980s. In Fig. 11b a common feature stands out (except for the northerly types CT7 and CT5): there is an increase in the percentage of warm nights within the clusters since the 1970s onwards. These results will be analysed more in depth in next section.

4. Discussion

The circulation classifications provide an insight into the SLP patterns more conducive to extreme temperatures for different regions and locations, and permit an analysis of fluctuations of extreme temperatures related to changes in the CTs frequency and within-type changes.

4.1. Changes in extreme temperatures related to circulation changes

The changes found in extreme temperature indices (Section 3.1) are consistent with previous studies, e.g., higher uptrends in warm days over the SW Iberia, Mediterranean area and North Spain have been identified on an annual scale by Rodriguez-Puebla et al. (2010), Brunet et al. (2007) and El Kenawy et al. (2011b). Moreover, our results add information on the seasonal scale, e.g., the increase in warm days is more notable over the NE (Ebro Valley) and South Iberia in summer and over central-western regions and Cantabrian Coast in spring (over the Mediterranean coast in both seasons). Trends detected in the spring and summer frequency of the CTs over the last two periods (1950–2003; 1970–2003) are in general agreement with those reported using other CTs classifications for Western Europe since the 1950s or the 1960s (Lorenzo et al., 2011; Esteban et al., 2006; see Section 1).

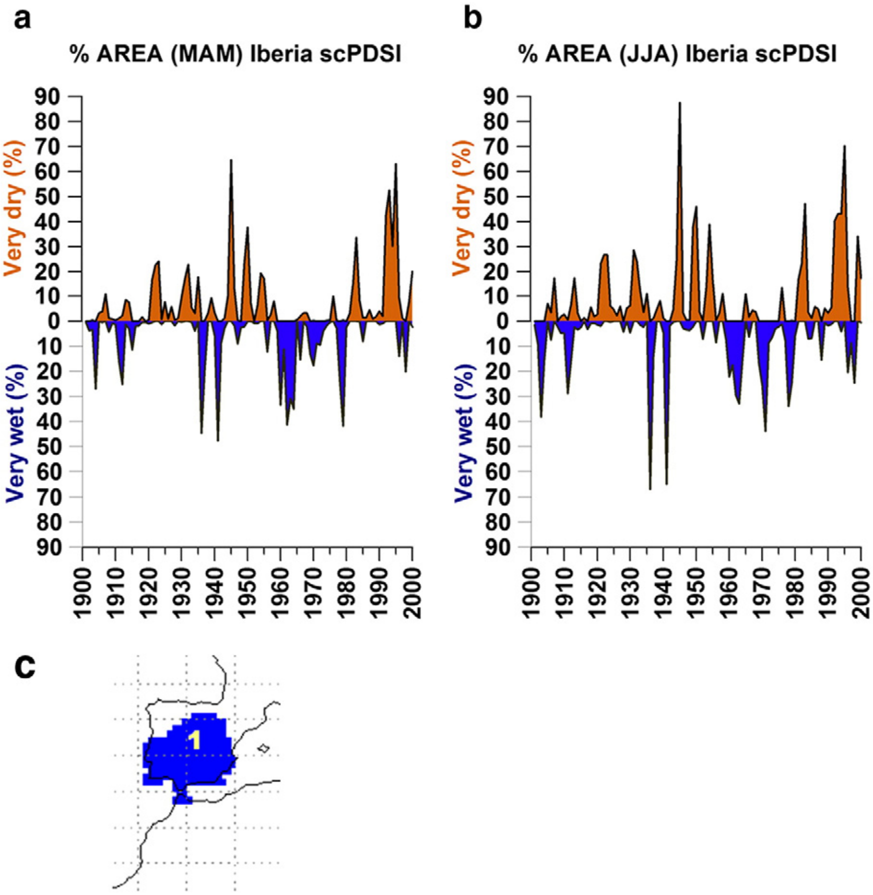

Fig. 12. Percentage (%) of Iberian area (defined in c) with very wet and dry conditions according to scPDSI drought index (Wells et al. 2001) for;. a) spring (MAM) b) summer (JJA) c) Iberian domain considered (adapted from Sousa et al., 2011). See van der Schrier et al. (2006) for the definiton of very dry/wet conditions according to scPDSI values.

Therefore, we can highlight some concordant signals in extreme temperature indices (Figs. 2 to 5) with respect to CTs frequency changes (Figs. 6–7, Tables 2–3), whose links have been exposed in previous Section 3.3 (Figs 8a–11a and Table 4):

- A decrease in the frequency of spring cold nights, which is notable in the 1970s onwards in whole Iberia is partially attributable to a downtrend in the frequency of northerly flow in 1970–2003 (CT5 Fig. 8a; Table 2). This stands especially for the Northern half (EOF1 in Fig. 2, Table 4a).
- An increase in spring warm days in West and North Iberia in the 1990s (EOF5 and EOF1 in Fig. 3) is related to increased frequencies of CT1 and, especially, CT8 (Fig. 6b, Fig. 9a).
- Spring warm days in the Southern Mediterranean region (EOF3, Fig 3) are related to SW type (CT9 and CT6 – Fig. 9a; Table 4a), with higher frequency in the 1950s and 1960s and moderate positive trend from 1970 to 2003 (Table 2).
- The increase in spring warm days over NE Cantabrian coast and Ebro Valley (EOF4, Fig. 3) is positively correlated with the frequency of stagnant situations over the IP with relative low pressure in North Atlantic region (therefore providing south component in the flow), such as CT4 and CT6 (Table 4a). Also warm conditions in this region are influenced by CT9 (Fig. 9a), but the steep increase in warm days around the 2000s (EOF4, Fig. 3) appear somehow decoupled from the frequency of this CT (Fig. 9b, red line in CT9).
- The notable increase in summer warm days to the NE (Fig. 4; EOF1) could be due to a high frequency of summer types CT1 and CT8 (Fig. 10a), although this is not supported by significant correlations (Table 4b).
- Increases in summer warm nights are notable (Fig. 5): To the SW (EOF4), they may be partially related to uptrends in North Atlantic Anticyclone with easterly flow (1850–2003); To the SE (EOF1), they are more related to Iberian thermal low patterns such as CT4 (Fig. 7, Fig. 11a) which exhibits a positive trend in 1950–2003 (Table 3). A further warming in Iberia would in fact lead to higher frequency of thermal lows, as projected by Hoinka et al. (2007) and Jerez et al. (2012).

4.2. Within-type changes: identification of other physical forcings

Within-type changes in the percentage of extremes are shown in Figs. 8b, 9b, 10b and 11b: A nearly constant extreme character (red line) implies a long-term stable relationship between CTs and extreme temperatures, and it would yield confidence in the above exposed relationships. In contrast, the existence of low-frequency within-type changes leads us to identify periods and regions in which other physical mechanisms

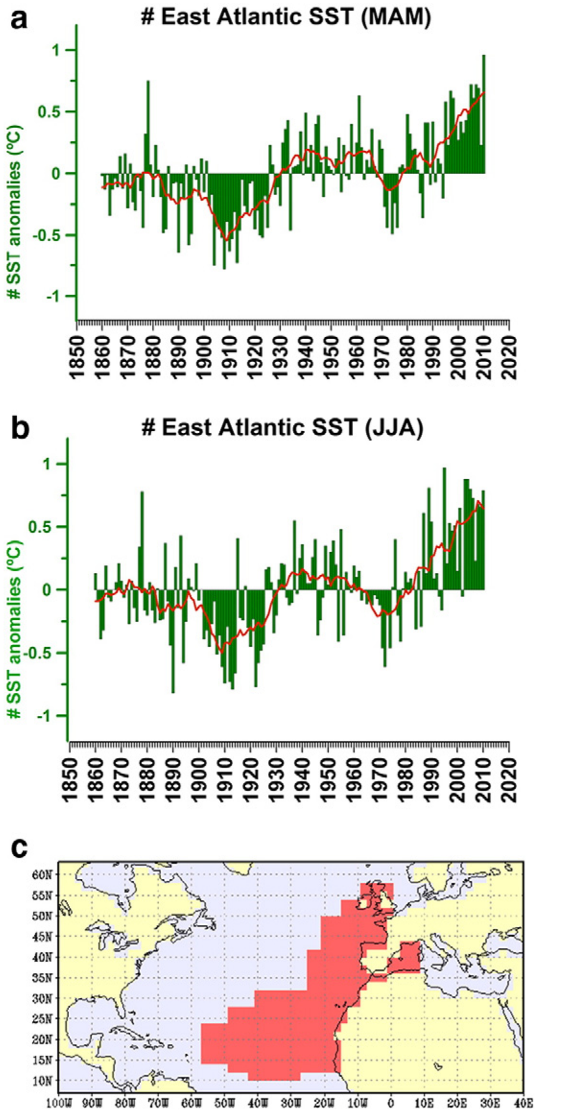

Fig. 13. In green bars, seasonal East Atlantic (EA) SSTs anomalies for the period 1860–2010 (red lines are 11-year moving averages). For a) spring (MAM) and b) summer (JJA). c) EA SST domain, as in Sousa et al. (2011) and Hertig and Jacobeit (2010). Data source: http://www.ncdc.noaa.gov/ersst/ (ERSST.v3b).

have clearly modulated the temperature within the CTs. A discussion of these results, and an overview presented in Table 5, is provided in the following.

Table 5a–b summarizes changes in average Tmax and Tmin within all the CTs for the whole period and two half-periods. Overall there are fewer trends in spring (i.e., there is more stability in the relationship circulation-temperature) than summer, which makes sense because summer temperatures are most affected by other factors besides SLP (El Kenawy et al., 2011a). In general uptrends in Tmax occurred throughout the whole century (especially in summer), whereas in the first half Tmin show fewer significant increases, in agreement with averaged Spanish series and trends shown by Brunet et al. (2007).

For 1954–2003, increases in summer Tmax and Tmin are comparable (Table 5b). However, 3 out of 8 summer CTs do not present significant changes in the second period 1954–2003 (CT3 and especially, CT5 and CT7, see Table 5b): they have in common a northerly flow component (from NW to NE), which can introduce cool air. The highest rates of warming are found for CT1, CT4 and CT8. For spring, the most remarkable trend is found within CT9, for the whole period, and especially in 1954–2003 (Tmax rate is 0.70 ± 0.22 °C/decade, i.e, about 3.5 °C in the total period, as is for CT6). A great increase in the frequency of warm days within CT9 (since mid-70s) is also evident from Fig. 9b (bottom panel). Summer CT8 and spring CT9 are the most "cyclonic" types, with W/SW flow component. The highest warming within these south-westerly types could reflect the importance both of heat advection processes (such as from Subtropical Atlantic Ocean/ Northern Africa) and of soil-atmosphere coupling throughout the Iberian plateau.

Therefore, the influence of SSTs on the variability of temperature extremes in the Iberian Peninsula must be considered (e.g., Della-Marta et al., 2007). During day-time both in spring and summer the oceans act as heat storage. When SST is very high then ocean surface will be able to absorb less heat from the atmosphere, being less effective in its role of *attenuation* of land temperatures. East Atlantic (EA) SSTs anomalies for spring and summer are shown in Fig. 13a–b. Internal variability of Atlantic Ocean caused a cold period in 1900 up to around 1930, followed by 30 years of relative warmth and another cold phase from 1960 to 1990, with a warming period since then (Ting et al., 2009). However, due to anthropogenic forcing added to the internal variability, the last raise in SSTs started earlier (Cattiaux et al., 2010), around the mid-1970s for the EA domain (see Fig. 13a–c).

Thus, low-frequency variations in the warm (and cold) character of some circulation types (Fig. 8b to 11b) are coincident with periods of strong anomalies in the EA SSTs: a remarkable increasing warm character over 1930 to around mid-1950s, and in the 1980s, is observed for prevailing westerly types (CT2 and 6 in spring, Fig. 9b; CT3 and CT8, summer Figs. 10–11b) coincident with positive EA SSTs anomalies (Fig. 13a–b). Also CTs with prevailing easterly flow (i.e., CT8 of spring and CT1, CT2, CT4 and CT6 of summer) show increased warm character from 1920 to 1950, decreasing warm character up to 1970s and increase since then, in agreement with EA SSTs anomalies (note that the domain includes Western Mediterranean, Fig. 13c). It is worth noting that, in contrast, northerly flow types exhibit less pronounced within-type change, such as for spring CT5 and CT3 (Fig. 8b, red line; Table 5a) and summer CT5 and CT7 (Fig. 11b; Table 5b). This is in agreement with a greater warming of the Atlantic Ocean south than 45º N (Solomon et al., 2007).

Some correlations (Table 4a-b) between regional extreme series (Figs. 2–5) and EA SST anomalies support this SST influence. It has sense that they stand especially for coastal regions and low lands in West Iberia opened to the Atlantic influence. Thus, there is a significant positive correlation between EA SST anomalies and summer warm nights in the SW Atlantic region (EOF4 in Fig. 5) and NE Mediterranean (EOF5). Also for spring warm days a positive correlation stands for the Mediterranean south region (rho = 0.41, EOF3 in Fig. 2) and West/Atlantic region (rho = 0.28, EOF5). During night time (in spring, as in autumn and winter) the atmosphere mostly absorbs heat from the sea surface. Hence, a negative association stands between cold nights series for the N/NE and EA SST (rho = −0.38, EOF1 in Fig. 3). This agrees with Rodriguez-Puebla et al. (2010) who found a significant contribution of SSTs on the decrease of annual cold nights in the IP.

In addition, as argued in Section 1, Tmax in transitional climate zones is substantially influenced by soil moisture availability. Therefore, it is natural that during periods of intense droughts in the IP, such as in mid-1940s to mid-1950s, mid 1980s, and remarkably the 1990s (see Fig. 12a–b), the frequency of within-type warm days increases, for spring (Fig. 9b, CT2 and CT6) and summer (Fig. 10b, CT1 and CT6). This is also observed in some of the regional series of extreme temperatures themselves (Figs. 3, 4). Indeed, there is a significant correlation (rho = 0.32, Table 4a) between Iberian area with very dry conditions in spring (scPDSI_dry) and the evolution of extreme warm days in the west-central part of Iberia (EOF1 in Fig 3). For summer (Table 4b), there is a higher significant correlation between the area with drought conditions and warm days series for central-south region (EOF2, rho = 0.36) and warm nights for W/SW region (EOF4, rho = 0.38). This agrees with regional simulations for the IP which have shown the primary influence of soil moisture on summer temperatures, particularly in central parts (Jerez et al., 2010).

Finally, for both spring (Fig. 9b) and summer (Fig. 10b), the number of warm days within the CTs increases remarkably in the 1980s. Besides the mentioned factors, this behaviour could be also influenced by changes in insolation over the IP that are somehow independent of changes in circulation. Indeed, some works have highlighted the so-called periods of "dimming" (around 1950s to 1980s) and "brightening" (mid-1980s to mid-2000´s) especially noticeable in spring and summer seasons for the IP (Sanchez-Lorenzo et al., 2007, 2008, 2009). The cited works attributed a large part of these changes in sunshine duration to radiative effects of aerosols (whose concentrations are reported to have been higher from 1950 to mid-1980s) and also to increases in cloudiness in the 1950s and 1960s. The latter is probably connected to circulation changes, e.g., consistent with a higher frequency of cyclonic types (summer-CT8 and spring-CT9) in those decades (Fig. 7b, 6b).

This work provides information about Iberian CTs-extreme temperatures relationships and low-frequency variations in these links. It is important to note that to develop statistical downscaling methods for daily extremes the usage of only a few characteristic circulation types is insufficient, since such a simplification reduces considerably both the day by day and the interannual variance. Therefore, for modelling high frequency changes in extremes and in order to perform both future projections and past reconstructions more synoptic detail is needed, such as methods based on circulation analogues (Brands et al., 2011; Cattiaux et al., 2011). Also the consideration of upper levels variability, e.g. 500 hPa geopotential heights – not available with high confidence for the period analysed – would probably improve the dynamic characterization (García-Herrera et al., 2005; Maheras et al., 2006). As well, from interannual to multidecadal time scales, the consideration of other predictors or forcing factors (SSTs, soil moisture, solar radiation) is probably necessary, even though they are somehow interconnected with each other and related with atmospheric dynamics at different scales.

5. Concluding remarks

The approach developed in this article takes the daily basis for the relationship between characteristic circulation types (CTs, 9 for spring and 8 for summer) and moderate extreme temperature indices for 29 stations in the IP.

Long-term changes in CTs frequency (1850–2003) indicate an uptrend in strong North Atlantic Anticyclone and downtrends in patterns with North Atlantic low pressure both in spring and summer.

Spatiotemporal variability in the seasonal occurrence of moderately extreme temperatures in Iberia can be attributed to some extent to changes in the frequency of the CTs. The notable changes in the frequency of extreme temperatures observed since the 1970s are consistent with some frequency changes in the CTs from 1970 to 2003: For spring, a downtrend in the frequency of northerly flow is related to less frequent cold nights in West and North Iberia; increasing frequency of south-westerly flow in this period (albeit less frequent than in previous past decades) is connected to an increase in warm days in the Southern half. As well, peaks of high frequency of Anticyclone in North Iberia in the 1980s and 1990s contributed to enhancing spring warm days to the north and west of Iberia.

In summer, a high frequency of the Anticyclone bridge (as in summer 2003) and Iberian thermal low patterns (positive trend over 1950–2003) have likely contributed to more summer warm days and nights respectively.

Within-type changes in the extreme character of the CTs have been analysed (1905–2003) in order to identify whether other physical factors have a signal on decadal timescales. Increases in Tmax, Tmin and warm extremes within most of the types are found, except for patterns associated with N/NE flow. Increases in the warm character of most of the types are detected in the 1980s onwards, in agreement with a reported solar "brightening" period in spring and summer in the IP. Furthermore, periods of warming/cooling of westerly and easterly CTs generally coincide with observed periods of increasing/decreasing East Atlantic (including Western Mediterranean) SSTs. The SST modulation stands especially for coastal regions. Decades with very dry conditions in Iberia (mid 1940s to 1950s, mid 1980s and 1990s) also correlate with increased frequency of warm days, particularly for central and southwest Iberia.

Based on observational data, our analysis highlights for a long-term perspective the importance of circulation changes and sea-air-land interactions to extreme temperatures in different regions of the Iberian Peninsula. The contribution of atmospheric dynamics has been comprehensively analysed, obtaining (as expected) a better characterization for spring than summer extreme temperatures. The influence of long-term memory physical factors (SST and dry soil conditions) on regional extreme temperature series has been analysed visually and by simple correlation tests, but it should be further studied, e.g. by means of climate model simulations.

Acknowledgments

S. Fernández-Montes and F.S. Rodrigo were supported by the Spanish Ministry of Education and Science (project

CGL2007-65546-C03-01) and the Junta de Andalucía (project GLOCHARID). S. Seubert was supported by the German Research Foundation (project KLIWEX-MED). P. M. Sousa work was supported by the 7th Framework Program project FUME (contract number 243888). The authors thank to E. Aguilar from the Climate Research Group of the University Rovira I Virgili (Tarragona, Spain) for providing the original temperature data series (SDATS) and the providers in the ECA&D project (http://eca.knmi.nl). As well we thank to COST733 action and A. Philipp (University of Augsburg) for providing the classification software. S. Fernández-Montes acknowledges the main scientific and institutional supports given by Jucundus Jacobeit (University of Augsburg) and Ricardo M. Trigo (University of Lisbon) during, respectively, the initial and final stages of this work.

References

Ansell, T., Jones, P.D., Allan, R.J., Lister, D., Parker, D.E., Brunet-India, M., Moberg, A., Jacobeit, J., Brohan, P., Rayner, N., Aguilar, E., Alexandersson, H., Barriendos, M., Brazdil, R., Brandsma, T., Cox, N., Drebs, A., Founda, D., Gerstengarbe, F., Hickey, K., Jonsson, T., Luterbacher, J., Nordli, O., Oesterle, H., Rodwell, M., Saladie, O., Sigro, J., Slonosky, V., Srnec, L., Suarez, A., Tuomenvirta, H., Wang, X., Wanner, H., Werner, P., Wheeler, D., Xoplaki, E., 2006. Daily mean sea level pressure reconstructions for the European–North Atlantic region for the period 1850–2003. J. Clim. 19, 2717–2742.

Barnston, A.G., Livezey, R.E., 1987. Classification, seasonality and persistence of low frequency atmospheric circulation patterns. Mon. Weather Rev. 115, 1083–1126.

Barriopedro, D., Fischer, E.M., Luterbacher, J., Trigo, R.M., García-Herrera, R., 2011. The hot summer of 2010: redrawing the temperature record map of Europe. Science 332, 220–224.

Beck, C., Jacobeit, J., Jones, P.D., 2007. Frequency and within-type variations of large scale circulation types and their effects on low-frequency climate variability in Central Europe since 1780. Int. J. Climatol. 27, 473–491.

Bermejo, M., Ancell, R., 2009. Observed changes in extreme temperatures over Spain during 1957–2002 using Weather Types. J. Climatol. 9, 45–61 ISSN 1578–8768.

Brands, S., Taboada, J.J., Cofiño, A.S., Sauter, T., Schneider, C., 2011. Statistical downscaling of daily temperatures in the NW Iberian Peninsula from global climate models: validation and future scenarios. Clim. Res. 48, 163–176.

Brunet, M., Saladié, O., Jones, P., Sigró, J., Aguilar, E., Moberg, A., Lister, D., Walther, A., Lopez, D., Almarza, C., 2006. The development of a new dataset of Spanish daily adjusted temperature series (SDATS) (1850–2003). Int. J. Climatol. 26, 1777–1802.

Brunet, M., Jones, P.D., Sigró, J., Saladié, O., Aguilar, E., Moberg, A., Della-Marta, P.M., Lister, D., Walther, A., López, D., 2007. Temporal and spatial temperature variability and change over Spain during 1850–2005. J. Geophys. Res. 112, D12117. http://dx.doi.org/10.1029/2006JD008249.

Brunet, M., Saladié, O., Jones, P.D., Sigró, J., Aguilar, E., Moberg, A., Lister, D., Walther, A., Almarza, C., 2008. A case-study/guidance on the development of long-term daily adjusted temperature datasets, WCDMP-66/WMO-TD-1425. WMO, Geneva, Switzerland. 43 pp.

Cassou, C., Terray, L., Phillips, A.S., 2005. Tropical Atlantic influence on European heat waves. J. Clim. 18 (15), 2805–2811.

Cattiaux, J., Vautard, R., Yiou, P., 2010. North-Atlantic SST amplified recent wintertime European land temperature extremes and trends. Clim. Dyn. 36 (11–12), 2113–2128. http://dx.doi.org/10.1007/s00382-010-0869-0.

Cattiaux, J., Yiou, P., Vautard, R., 2011. Dynamics of future seasonal temperature trends and extremes in Europe: a multi-model analysis from CMIP3. Clim. Dyn. http://dx.doi.org/10.1007/s00382-011-1211-1.

Della-Marta, P.M., Luterbacher, J., von Weissenfluh, H., Xoplaki, E., Brunet, M., Wanner, H., 2007. Summer heat waves over western Europe 1880–2003, their relationship to large-scale forcings and predictability. Clim. Dyn. 29 (2–3), 251–275.

Domonkos, P., Kysely, J., Piotrowicz, K., Petrovic, P., Likso, T., 2003. Variability of extreme temperature events in South-Central Europe during the 20th century and its relationship with large-scale circulation. Int. J. Climatol. 23, 987–1010.

El Kenawy, A., López-Moreno, I., Vicente-Serrano, S.M., 2011a. Trend and variability of temperature in northeastern Spain (1920–2006): linkage to atmospheric circulation. Atmos. Res. 106, 159–180.

El Kenawy, A., López-Moreno, J.I., Vicente-Serrano, S.M., 2011b. Recent trends in daily temperature extremes over northeastern Spain (1960–2006). Nat. Hazard. Earth Syst. Sci. 11, 2583–2603. http://dx.doi.org/10.5194/nhess-11-2583-2011.

Esteban, P., Martin-Vide, J., Mases, M., 2006. Daily atmospheric circulation catalogue for western europe using multivariate techniques. Int. J. Climatol. 26, 1501–1515.

Esteban, P., Ninyerola, M., Prohom, M., 2009. Spatial modelling of air temperature and precipitation for Andorra (Pyrenees) from daily circulation patterns. Theor. Appl. Climatol. 96, 43–56.

Fernández-Montes, S., Rodrigo, F.S., 2011. Trends in seasonal indices of daily temperature extremes in the Iberian Peninsula, 1929–2005. Int. J. Climatol. 31. http://dx.doi.org/10.1002/joc.3399.

Fernández-Montes, S., Seubert, S., Rodrigo, F.S., Hertig, E., 2012. Wintertime circulation types over the Iberian Peninsula: long-term variability and relationships with weather extremes. Clim. Res. 53, 205–227. http://dx.doi.org/10.3354/cr01095.

Ferranti, L., Viterbo, P., 2005. The European summer of 2003: sensitivity to soil water initial conditions. J. Climate 19, 3659–3680.

Feudale, L., Shukla, J., 2010. Influence of sea surface temperature on the European heat wave of 2003 summer. Part I: an observational study. Clim. Dyn. http://dx.doi.org/10.1007/s00382-010-0788-0.

García-Herrera, R., Díaz, J., Trigo, R.M., Hernández, E., 2005. Extreme summer temperatures in Iberia: health impacts and associated synoptic conditions. Ann. Geophys. 23, 239–251.

Goodess, C., Jones, P., 2002. Links between circulation and changes in the characteristics of Iberian rainfall. Int. J. Climatol. 22, 1593–1615.

Hertig, E., Jacobeit, J., 2010. Predictability of Mediterranean climate variables from oceanic variability. Part I: Sea surface temperature regimes. Clim. Dyn. http://dx.doi.org/10.1007/s00382-010-0819-x.

Hoinka, K.P., Gaertner, M., de Castro, M., 2007. Iberian thermal lows in a changed climate. Q. J. R. Meteorol. Soc. 133 (626 A), 1113–1126.

Huth, R., Beck, C., Philipp, A., Demuzere, M., Ustrnul, Z., Cahynová, M., Kysely´, J., Tveito, O.E., 2008. Classifications of atmospheric circulation patterns: recent advances and applications. Ann. N. Y. Acad. Sci. 1146, 105–152.

Jacobeit, J., Wanner, H., Luterbacher, J., Beck, C., Philipp, A., Sturm, K., 2003. Atmospheric circulation variability in the North Atlantic- European area since the mid-seventeenth century. Clim. Dyn. 20, 341–352.

Jacobeit, J., Rathmann, J., Philipp, A., Jones, P.D., 2009. Central European precipitation and temperature extremes in relation to large-scale atmospheric circulation types. Meteorol. Z. 18, 397–410.

Jerez, S., Montavez, J.P., Gomez-Navarro, J.J., Jimenez-Guerrero, P., Jimenez, J., Gonzalez-Rouco, J.F., 2010. Temperature sensitivity to the land-surface model in MM5 climate simulations over the Iberian Peninsula. Meteorol. Z. 19 (4), 363–374.

Jerez, S., Montavez, J.P., Gomez-Navarro, J.J., Jimenez, P.A., Jimenez-Guerrero, P., Lorente, R., Gonzalez-Rouco, J.F., 2012. The role of the land-surface model for climate change projections over the Iberian Peninsula. J. Geophys. Res. 117, D01109. http://dx.doi.org/10.1029/2011JD016576.

Jones, P.D., Lister, D.H., 2009. The influence of the circulation on surface temperature and precipitation patterns over Europe. Clim. Past Discuss. 5, 535–555. http://dx.doi.org/10.5194/cpd-5-535-2009.

Kendall, M.G., 1938. A new measure of rank correlation. Biometrika 30, 81–93.

Klein Tank, A.M.G., et al., 2002. Daily dataset of 20th-century surface air temperature and precipitation series for the European Climate Assessment. Int. J. Climatol. 22, 1441–1453.

Klok, E.J., Klein Tank, A.M.G., 2009. Updated and extended European dataset of daily climate observations. Int. J. Climatol. 29 (8), 1182–1191.

Küttel, M., Luterbacher, J., Wanner, H., 2010. Multidecadal changes in winter circulation-climate relationship in Europe: frequency variations, within-type modifications, and long-term trends. Clim. Dyn. http://dx.doi.org/10.1007/s00382-009-0737-y.

Lorenzo, M.N., Taboada, J.J., Gimeno, L., 2008. Links between circulation weather types and teleconnection patterns and their influence on precipitation patterns in Galicia (NW Spain). Int. J. Climatol. 28, 1493–1505.

Lorenzo, M.N., Ramos, A.M., Taboada, J.J., Gimeno, L., 2011. Changes in Present and Future Circulation Types Frequency in Northwest Iberian Peninsula. PloS one 6 (1), e16201. http://dx.doi.org/10.1371/journal.pone.0016201.

Maheras, P., Flokas, H., Tolika, K., Anagnostopoulou, C., Vafiadis, M., 2006. Circulation types and extreme temperature changes in Greece. Clim. Res. 30, 161–174.

Moberg, A., Jones, P., Lister, D., Walther, A., Brunet, M., Jacobeit, J., Alexander, L., Della-Marta, P., Luterbacher, J., Yiou, P., Chen, D., Klein Tank, A., Saladié, O., Sigró, J., Aguilar, E., Alexandersson, H., Almarza, C., Auer, I., Barriendos, M., Begert, M., Bergström, H., Böhm, R., Butler, C.J., Caesar, J., Drebs, A., Founda, D., Gerstengarbe, F., Micela, G., Maugeri, M., Österle, H., Pandzic, K., Petrakis, M., Srnec, L., Tolasz, R., Tuomenvirta, H., Werner, P., Linderholm, H., Philipp, A., Wanner, H., Xoplaki, E., 2006. Indices for daily temperature and precipitation extremes in Europe analyzed for the period 1901–2000. J. Geophys. Res. 111 (D22), 106.

Philipp, A., Della-Marta, P.M., Jacobeit, J., Fereday, D., Jones, P., Moberg, A., Wanner, H., 2007. Long-term variability of daily North Atlantic–European

pressure patterns since 1850 classified by simulated annealing clustering. J. Clim. 20, 4065–4095.
Preisendorfer, R., 1988. Principal Component Analysis in Meteorology and Oceanography. Developments in Atmospheric Science, vol. 17. Elsevier, Amsterdam.
Ramos, A.M., Ramos, R., Sousa, P., Trigo, R.M., Janeira, M., Prior, V., 2011a. Cloud to ground lightning activity over Portugal and its association with Circulation Weather Types. Atmos. Res. 101, 84–101. http://dx.doi.org/10.1016/j.atmosres.2011.01.
Ramos, A.M., Trigo, R.M., Santo, F.E., 2011b. Evolution of extreme temperatures over Portugal: recent changes and future scenarios. Clim. Res. 48, 177–192. http://dx.doi.org/10.3354/cr00934 1088.
Rasilla, D.F., 2003. Aplicación de un método de clasificación sinóptica a la Península Ibérica. Investig. Geogr. 30, 27–44.
Rasilla, D.F., García-Codron, J.C., Carracedo, V., Diego, C., 2010. Circulation patterns, wildfire risk and wildfire occurrence in continental Spain. Phys. Chem. Earth. 35, 553–560 (1092).
Rodriguez-Puebla, C., Encinas, A.H., García-Cansado, L.A., Nieto, S., 2010. Trends in warm days and cold nights over the Iberian Peninsula: relationships to large-scale variables. Clim. Change 100, 667684. http://dx.doi.org/10.1007/s10584-009-9721.0.
Sanchez-Lorenzo, A., Brunetti, M., Calbo´, J., Martin-Vide, J., 2007. Recent spatial and temporal variability and trends of sunshine duration over the Iberian Peninsula from a homogenized data set. J. Geophys. Res. 112, D20115. http://dx.doi.org/10.1029/2007JD008677.
Sanchez-Lorenzo, A., Calbo´, J., Martin-Vide, J., 2008. Spatial and temporal trends in sunshine duration over Western Europe (1938 –2004). J. Clim. 21, 6089–6098. http://dx.doi.org/10.1175/2008JCLI2442.1.
Sanchez-Lorenzo, A., Calbo, J., Brunetti, M., Deser, C., 2009. Dimming/brightening over the Iberian Peninsula: Trends in sunshine duration and cloud cover, and their relations with atmospheric circulation. J. Geophys. Res. 114, D00D09. http://dx.doi.org/10.1029/2008JD011394.
Schar, C., Vidale, P.L., Luthi, D., Frei, C., Haberli, C., Liniger, M.A., Appenzeller, C., 2004. The role of increasing temperature variability in the European summer heatwaves. Nature 427, 332–336.
Seneviratne, S.I., Corti, T., Davin, E.L., Hirschi, M., Jaeger, E.B., Lehner, I., Orlowsky, B., Teuling, A.J., 2010. Investigating soil moisture-climate interactions in a changing climate: A review. Earth Sci. Rev. 99 (3–4), 125–161. http://dx.doi.org/10.1016/j.earscirev.2010.02.004.
Slonosky, V., Jones, P., Davies, T., 2001. Atmospheric circulation and surface temperature in Europe from the 18th century to 1995. Int. J. Climatol. 21, 63–75. http://dx.doi.org/10.1002/joc.591.
Smith, T.M., Reynolds, R.W., Peterson, T.C., Lawrimore, J., 2008. Improvements to NOAA's Historical Merged Land-Ocean Surface Temperature Analysis (1880–2006). J. Clim. 21, 2283–2296.
Solomon, S., Qin, D., Manning, M., Chen, Z., Marquis, M., Averyt, K.B., Tignor, M., Miller, H.L., 2007. *Climate Change 2007: The Physical Science Basis*, Contribution of Working Group I to the Fourth Assessment Report of the Intergovernmental Panel on Climate Change. Cambridge University Press: Cambridge, United Kingdom and New York, NY, USA.
Sousa, P.M., Trigo, R.M., Aizpurua, P., Nieto, R., Gimeno, L., Garcia-Herrera, R., 2011. Trends and extremes of drought indices throughout the 20th century in the Mediterranean. Nat. Hazard. Earth Syst. Sci. 11, 33–51. http://dx.doi.org/10.5194/nhess-11-33-2011.
Ting, M., Kushnir, Y., Seager, R., Li, C., 2009. Forced and internal twentieth-century SST trends in the north Atlantic. J. Clim. 22 (6), 1469–1481.
Trigo, R.M., DaCamara, C.C., 2000. Circulation weather types and their impact on the precipitation regime in Portugal. Int. J. Climatol. 20, 1559–1581.
Trigo, I.F., Davies, T.D., Bigg, G.R., 1999. Objective climatology of cyclones in the Mediterranean region. J. Clim. 12, 1685–1696.
Trigo, R.M., Pereira, J.M.C., Pereira, M.G., Mota, B., Calado, T.J., Dacamara, C.C., Santo, F.E., 2006. Atmospheric conditions associated with the exceptional fire season of 2003 in Portugal. Int. J. Climatol. 26 (13), 1741–1757.
van der Schrier, G., Briffa, K.R., Jones, P.D., Osborn, T.J., 2006. Summer moisture variability across Europe. J. Clim. 19, 2818–2834.
Wells, N., Goddard, S., Hayes, M.J., 2004. A self-calibrating Palmer Drought Severity Index. J. Clim. 17, 2335–2351.
Xoplaki, E., González-Rouco, J.F., Luterbacher, J., Wanner, H., 2003. Mediterranean summer air temperature variability and its connection to the large scale atmospheric circulation and SSTs. Clim. Dyn. 20, 723–739.
Zampieri, M., D'Andrea, F., et al., 2009. Hot European summer and the role of soil moisture in the propagation of Mediterranean drought. J. Clim. 22 (18), 4747–4758. http://dx.doi.org/10.1175/2009JCLI2568.1.